

ISTANBUL TECHNICAL UNIVERSITY ★ GRADUATE SCHOOL

**MODELLING VOLATILITY DYNAMICS OF CRYPTOCURRENCIES:
A COMPARISON OF
GARCH AND STOCHASTIC VOLATILITY MODELS**

M.A. THESIS

İrfan Caner KAYA

Department of Economics

Economics M.A. Program

JUNE 2025

ISTANBUL TECHNICAL UNIVERSITY ★ GRADUATE SCHOOL

**MODELLING VOLATILITY DYNAMICS OF CRYPTOCURRENCIES:
A COMPARISON OF
GARCH AND STOCHASTIC VOLATILITY MODELS**

M.A. THESIS

**İrfan Caner KAYA
(412221005)**

Department of Economics

Economics M.A. Program

Thesis Advisor: Assoc. Prof. Dr. Osman DOĞAN

JUNE 2025

İSTANBUL TEKNİK ÜNİVERSİTESİ ★ LİSANSÜSTÜ EĞİTİM ENSTİTÜSÜ

**KRİPTO PARALARIN VOLATİLİTE DİNAMİKLERİNİN
MODELLENMESİ: GARCH VE STOKASTİK VOLATİLİTE
MODELLERİNİN KARŞILAŞTIRILMASI**

YÜKSEK LİSANS TEZİ

**İrfan Caner KAYA
(412221005)**

İktisat Anabilim Dalı

İktisat Tezli Yüksek Lisans Programı

Tez Danışmanı: Doç. Dr. Osman DOĞAN

HAZİRAN 2025

İrfan Caner KAYA, an M.A. student of ITU Department of Economics student ID 412221005 successfully defended the thesis entitled “MODELLING VOLATILITY DYNAMICS OF CRYPTOCURRENCIES: A COMPARISON OF GARCH AND STOCHASTIC VOLATILITY MODELS”, which he/she prepared after fulfilling the requirements specified in the associated legislations, before the jury whose signatures are below.

Thesis Advisor : **Assoc. Prof. Dr. Osman DOĞAN**
Istanbul Technical University

Jury Members : **Assoc. Prof. Dr. Mete Han YAĞMUR**
Istanbul Technical University

Assist. Prof. Dr. Mahmut Sami GÜNGÖR
Marmara University

.....

Date of Submission : **30 May 2025**

Date of Defense : **26 June 2025**





To my mother,



FOREWORD

First and foremost, I would like to express my deepest gratitude to my advisor, Assoc. Dr. Osman Dođan, whose continuous support, insightful guidance, and encouragement were invaluable throughout my M.A. in Economics at Istanbul Technical University. His mentorship not only deepened my understanding of econometric modeling but also inspired a lasting passion for academic research.

Pursuing a graduate degree in economics after years of studying Industrial Engineering was both a challenging and enriching journey. Balancing this academic endeavor with my professional responsibilities at TÜBİTAK was demanding, yet it proved to be a highly rewarding experience.

I am also sincerely thankful to all the lecturers at Istanbul Technical University. Their teachings broadened my perspective on economics, both in theory and in practice, and contributed significantly to my academic development.

Finally, I am deeply grateful to my mother, whose unwavering support and belief in me have been a source of strength throughout this journey.

June 2025

İrfan Caner KAYA

TABLE OF CONTENTS

	<u>Page</u>
FOREWORD	ix
TABLE OF CONTENTS	xi
ABBREVIATIONS	xiii
SYMBOLS	xv
LIST OF TABLES	xvii
LIST OF FIGURES	xx
SUMMARY	xxi
ÖZET	xxiii
1. INTRODUCTION	1
2. CRYPTO MARKET STRUCTURE AND FUNDAMENTALS OF CRYPTOCURRENCIES	5
2.1 Types of Cryptocurrencies	6
2.1.1 Payment Cryptocurrencies	6
2.1.2 Utility Tokens	7
2.1.3 Stablecoins	7
2.1.4 Central Bank Digital Currencies (CBDCs)	7
2.2 Cryptocurrencies Supply and Demand Dynamics	7
3. LITERATURE REVIEW	9
4. EMPIRICAL RESULTS	13
4.1 Data	13
4.2 Models	16
4.2.1 GARCH Models	16
4.2.2 Stochastic Volatility Models	22
4.3 Bayesian Estimation Method	25
4.3.1 Gibbs Sampler	25
4.3.2 Priors	26
4.3.3 Comparison of Models	28
4.4 Comparison of Volatility Models	30
4.5 Estimation Results	31
5. FORECASTING RESULTS	45
6. CONCLUSION	49
CURRICULUM VITAE	57



ABBREVIATIONS

AIC	: Akaike Information Criterion
BIC	: Bayesian Information Criterion
HQ	: Hannan-Quinn Information Criterion
AR	: Autoregressive Model
AR(1)	: First-Order Autoregressive Process
ARCH	: Autoregressive Conditional Heteroskedasticity
GARCH	: Generalized Autoregressive Conditional Heteroskedasticity
SV	: stochastic volatility model where h_t follows a stationary AR(1)
ACGARCH	: Asymmetric Component GARCH
CGARCH	: Component GARCH
EGARCH	: Exponential GARCH
TGARCH	: Threshold GARCH
APARCH	: Asymmetric Power ARCH
AVGARCH	: Asymmetric Absolute Value GARCH
IGARCH	: Integrated GARCH
HAR	: Heterogeneous Autoregressive Model
PCA	: Principal Component Analysis
PGARCH	: Power GARCH
FIGARCH	: Fractionally Integrated GARCH
FIEGARCH	: Fractionally Integrated EGARCH
MSGARCH	: Markov-Switching GARCH
ST-GARCH	: Smooth Transition GARCH
BTC	: Bitcoin
ETH	: Ether-the Native Cryptocurrency Token used by the Ethereum Network
BF	: Bayes Factor
SEC	: U.S. Securities and Exchange Commission
DApps	: Decentralized Applications
ETFs	: Exchange-Traded Funds
NFT	: Non-Fungible Token

CBDC	: Central Bank Digital Currency
P2P	: Peer-to-peer
XRP	: The Native Currency of The Ripple Network
DAO	: Decentralized Autonomous Organization
USDT	: Tether
BNB	: Binance Coin
KCS	: Kucoin Token
BAT	: Basic Attention Token
SOL	: Solana
DeFi	: Decentralized Finance
MCMC	: Markov Chain Monte Carlo
VaR	: Value at Risk
GHSKT	: Generalized Hyperbolic Skew Student's t
MCS	: Model Confidence Set
MSE	: Mean Squared Error
MAE	: Mean Absolute Error
MAPE	: Mean Absolute Percentage Error
QL	: Quantile Loss
ES	: Expected Shortfall
QAR	: Quantile Autoregressive Model
FOMO	: Fear of Missing Out
nig	: Normal Inverse Gaussian Distribution
ged	: Generalized Error Distribution
snorm	: Skewed Normal Distribution
sstd	: Skewed Student's t distribution
ghyp	: Generalized Hyperbolic Distribution
jsu	: Johnson's SU-distribution

SYMBOLS

μ	: mean return in standard GARCH(1,1) model
ε	: the innovation (residual, error or shock term) in standard GARCH(1,1) model
z_t	: an independent and identically distributed series of standardized white noises in the standard GARCH(1,1) model
α_0	: base level of volatility in standard GARCH(1,1) model
α_1	: measures the impact of the shocks in standard GARCH(1,1) model
β_1, β_2	: reflects the persistence levels in standard GARCH models
σ_t	: conditional volatility in GARCH models
σ_t^2	: conditional variance in GARCH models
q_t	: jump variable in GARCH-J and SV-J model
k_t	: jump size in GARCH-J and SV-J model
κ	: jump parameter in GARCH-J and SV-J model
μ_k	: average of the jump size of k_t
σ_k^2	: variance of the jump size of k_t
λ	: the volatility feedback parameter in GARCH-M and SV-M models
ψ	: moving average parameter in GARCH-MA model
ν	: the degree of freedom parameter in GARCH-t and SV-t models
δ_1	: the leverage effect parameter in GARCH-GJR model
$Q(20)$: Ljung-Box Statistics
$Q^2(20)$: McLeod-Li Statistics
h_t	: log-volatility of standard Stochastic Volatility (SV) model
μ_h	: unconditional mean of the volatility process
ϕ_h	: persistency of volatility in SV models
ε_t^h	: shock to the log-volatility in SV models
e_t^h	: time varying conditional variance
ε_t^y	: innovation term at time t in SV models
ω_h^2	: the variance of the error term in the log-volatility equation
ρ_h	: second-order autocorrelation in SV-2 model
ρ	: leverage effect parameter in SV-L model



LIST OF TABLES

	<u>Page</u>
Table 4.1: Statistical Summary of Bitcoin and Ethereum Daily Close Prices.....	15
Table 4.2: The List of GARCH and Stochastic Volatility Models.	25
Table 4.3: Log Marginal Likelihoods of the GARCH and SV Models of Bitcoin and Ethereum.	30
Table 4.4: Posterior means and Posterior standard deviations (in parentheses) for GARCH models: Bitcoin.	34
Table 4.5: Posterior means and Posterior standard deviations (in parentheses) for SV models: Bitcoin.	35
Table 4.6: Posterior means and Posterior standard deviations (in parentheses) for GARCH models: Ethereum.....	36
Table 4.7: Posterior means and Posterior standard deviations (in parentheses) for SV models: Ethereum.....	37
Table 5.1: Log Predictive Results of the GARCH and SV Models of Bitcoin and Ethereum	46



LIST OF FIGURES

	<u>Page</u>
Figure 4.1: Bitcoin Daily Closure Prices.	14
Figure 4.2: Ethereum Daily Closure Prices.....	14
Figure 4.3: The Daily Return Graph of Bitcoin.	17
Figure 4.4: The Correlogram of Daily Return of Bitcoin.	17
Figure 4.5: The Daily Return Squares Graph of Bitcoin.....	17
Figure 4.6: The Correlogram of Daily Return Squares of Bitcoin.	17
Figure 4.7: The Daily Absolute Return Graph of Bitcoin.	18
Figure 4.8: The Correlogram of Daily Absolute Return of Bitcoin.	18
Figure 4.9: The Daily Return Graph of Ethereum.	18
Figure 4.10: The Correlogram of Daily Return of Ethereum.	18
Figure 4.11: The Daily Return Squares Graph of Ethereum.	19
Figure 4.12: The Correlogram of Daily Return Squares of Ethereum.....	19
Figure 4.13: The Daily Absolute Return Graph of Ethereum.....	19
Figure 4.14: The Correlogram of Absolute Return of Ethereum.	19
Figure 4.15: Return Volatility Graph of Bitcoin: Standard GARCH Model.	38
Figure 4.16: Return Volatility Graph of Bitcoin: GARCH-2 Model.	38
Figure 4.17: Return Volatility Graph of Bitcoin: GARCH-J Model.....	38
Figure 4.18: Return Volatility Graph of Bitcoin: GARCH-M Model.	38
Figure 4.19: Return Volatility Graph of Bitcoin: GARCH-MA Model.	39
Figure 4.20: Return Volatility Graph of Bitcoin: GARCH-GJR Model.....	39
Figure 4.21: Return Volatility Graph of Bitcoin: Standard SV Model.	39
Figure 4.22: Return Volatility Graph of Bitcoin: SV-2 Model.....	39
Figure 4.23: Return Volatility Graph of Bitcoin: SV-J Model.	40
Figure 4.24: Return Volatility Graph of Bitcoin: SV-M Model.....	40
Figure 4.25: Return Volatility Graph of Bitcoin: SV-MA Model.....	40
Figure 4.26: Return Volatility Graph of Bitcoin: SV-L Model.....	40
Figure 4.27: Return Volatility Graph of Ethereum: Standard GARCH Model.....	41
Figure 4.28: Return Volatility Graph of Ethereum: GARCH-M Model.....	41
Figure 4.29: Return Volatility Graph of Ethereum: GARCH-MA Model.....	41
Figure 4.30: Return Volatility Graph of Ethereum: GARCH-t Model.	41
Figure 4.31: Return Volatility Graph of Ethereum: GARCH-GJR Model.	42
Figure 4.32: Return Volatility Graph of Ethereum: Standard SV Model.....	42
Figure 4.33: Return Volatility Graph of Ethereum: SV-2 Model.	42
Figure 4.34: Return Volatility Graph of Ethereum: SV-J Model.....	42
Figure 4.35: Return Volatility Graph of Ethereum: SV-M Model.	43
Figure 4.36: Return Volatility Graph of Ethereum: SV-MA Model.	43

Figure 4.37: Return Volatility Graph of Bitcoin: GARCH-t Model. 43
Figure 4.38: Return Volatility Graph of Bitcoin: SV-t Model. 43
Figure 4.39: Return Volatility Graph of Ethereum: GARCH-J Model. 44
Figure 4.40: Return Volatility Graph of Ethereum: SV-t Model. 44



MODELLING VOLATILITY DYNAMICS OF CRYPTOCURRENCIES: A COMPARISON OF GARCH AND STOCHASTIC VOLATILITY MODELS

SUMMARY

Cryptocurrencies have gained popularity since the invention of Bitcoin by Nakamoto. Although they lack regulation and carry a high risk of financial loss, they offer significant advantages, such as accessibility to the public, private transactions, decentralization, and diversified investment portfolios. One of the most distinguishing characteristics of cryptocurrencies is their high price volatility, which is significantly greater than that observed in traditional financial markets such as stocks or bonds. High volatility presents both opportunities and challenges for various stakeholders, including researchers, investors, financial analysts, risk managers, and policymakers. Moreover, as of March 11, 2025, the growing significance of cryptocurrencies in the global financial system is underscored by their combined market capitalization, which has exceeded 2.67 trillion US dollars. Hence, understanding and accurately modeling cryptocurrency volatility is crucial for making good investment decisions and developing robust risk management strategies. In this study, we focus on the volatility of the two largest cryptocurrencies by market capitalization: Bitcoin and Ethereum. We compare seven Generalized Autoregressive Conditional Heteroskedasticity (GARCH) models and seven Stochastic Volatility (SV) models using a Bayesian approach, based on the daily closing prices of Bitcoin and Ethereum.

We compute daily returns using closing prices sourced from cryptoQuotes, which provides open-access cryptocurrency market data, sentiment indicators, and interactive charts. The data covers the period from "19.10.2017 03:00" to "28.02.2025 03:00." for both Bitcoin and Ethereum. For each cryptocurrency, a total of 2683 observations are considered.

We consider the following models: the standard GARCH(1,1) and SV with first order autoregressive (AR(1)) log-volatility process, as well as their more flexible variants-including jump components (GARCH-J, SV-J), volatility-in mean versions (GARCH-M, SV-M), versions with moving average innovations (GARCH-MA, SV-MA), versions with t-distributed innovations (GARCH-t, SV-t), and version that allow for leverage effects (GARCH-GJR, SV-L). We also consider GARCH(2,1) and SV with second order autoregressive (AR(2)) log-volatility process (GARCH-2, SV-2).

In this thesis, we aim to compare the performance of these volatility models across two dimensions: estimation accuracy and forecasting performance.

For the estimation part, we evaluate the the goodness of fits of the GARCH and SV models to the daily closing returns of Bitcoin and Ethereum. Using a Bayesian technique, we compute the log-marginal likelihood of each model and calculate the posterior means of the model parameters. Our results show that SV-t is the best model

for both Bitcoin and Ethereum, with SV models generally outperforming GARCH counterparts. GARCH-t ranks second, showing the benefit of t -innovations. While the jump component enhances the estimation performance of the standard GARCH model for both Bitcoin and Ethereum, it does not have a significant impact on the standard SV model for Ethereum. For Bitcoin, the AR(2) specification underperforms compared to AR(1) process, whereas for Ethereum, AR(2) process demonstrates superior performance. The moving average component improves the estimation performance of Ethereum's SV model. The volatility feedback parameter in the volatility in mean models is statistically insignificant. Incorporating the leverage effect in the GARCH-GJR model enhances the performance over the standard GARCH specification, while it remains largely irrelevant in the SV models. Likewise, for Ethereum price returns, the leverage effect parameter is found to be statistically insignificant.

In our forecasting evaluation, we employ the log-predictive score to assess model performance. The results reveal distinct patterns across cryptocurrencies: the GARCH-t model demonstrates superior forecasting accuracy for Bitcoin, while GARCH-J performs best for Ethereum. We find that incorporating an AR(2) specification improves the Stochastic Volatility (SV) model's performance exclusively for Bitcoin. The inclusion of jump components significantly enhances forecasting accuracy for both standard GARCH and SV models in Bitcoin price returns. For Ethereum, jump components substantially improve the standard GARCH model while providing more modest gains to the baseline SV specification. The volatility feedback channel, as incorporated in both GARCH-M and SV-M models, plays a significant role in forecasting Bitcoin price returns, whereas it proves to be unnecessary for forecasting Ethereum price returns. The moving average innovations enhance the forecasting performance of the standard SV model for Bitcoin. Additionally, they yield minor improvements in the forecast accuracy of GARCH models for both cryptocurrencies and SV models for Ethereum. The inclusion of t -distributed innovations contributes to enhanced forecasting accuracy. Leverage effect benefits Bitcoin in GARCH and SV models but is insignificant for Ethereum.

KRİPTO PARALARIN VOLATİLİTE DİNAMİKLERİNİN MODELLENMESİ: GARCH VE STOKASTİK VOLATİLİTE MODELLERİNİN KARŞILAŞTIRILMASI

ÖZET

Kripto paralar, Nakamoto tarafından ortaya konan ilk örnek olan Bitcoin'in icadıyla birlikte finansal piyasalarda önemli bir yer edinmeye başlamıştır. Bu varlıklar, düzenleyici denetime tabi olmamaları ve yüksek düzeyde finansal risk barındırmaları nedeniyle eleştirilmekle birlikte; halka açık erişim, işlem gizliliği, merkeziyetsizlik ilkesi ve yatırım portföylerinin çeşitlendirilmesine olanak sağlamaları gibi çeşitli avantajlar sunmaktadır. Kripto paraların en belirgin özelliklerinden biri, hisse senetleri ve tahviller gibi geleneksel finansal araçlara kıyasla çok daha yüksek düzeyde fiyat oynaklığı sergilemeleridir. Bu yüksek oynaklık, yatırımcılar, analiz uzmanları, risk yöneticileri, araştırmacılar ve düzenleyici otoriteler için hem fırsatlar hem de zorluklar barındırmaktadır. Ayrıca, 11 Mart 2025 itibarıyla, kripto paraların küresel finansal sistemdeki artan önemi, toplam piyasa değerlerinin 2,67 trilyon Amerikan dolarını aşmasıyla vurgulanmaktadır. Dolayısıyla, kripto para piyasalarındaki oynaklığın doğru şekilde modellenmesi, sağlıklı yatırım kararlarının alınması ve etkin risk yönetimi stratejilerinin geliştirilmesi açısından büyük önem taşımaktadır.

Bu çalışmada, piyasa değeri bakımından en büyük iki kripto para birimi olan Bitcoin ve Ethereum'un oynaklık yapıları incelenmiştir. İki para birimine ait günlük kapanış fiyatları kullanılarak yedi farklı Genelleştirilmiş Otoregresif Koşullu Değişen Varyans (GARCH) modeli ile yedi farklı Stokastik Oynaklık (SV) modeli, Bayesyen yaklaşım kapsamında karşılaştırılmıştır.

Günlük getiriler, açık erişimli veri sağlayıcısı tarafından sunulan kapanış fiyatları kullanılarak hesaplanmıştır. Veri seti, hem Bitcoin hem de Ethereum için 19 Ekim 2017 ile 28 Şubat 2025 tarih aralığını kapsamaktadır. Her bir kripto para birimi için 2.683 gözlem yer almaktadır.

İncelenen modeller arasında temel GARCH(1,1) ve birinci dereceden otoregresif log-oynaklık sürecine sahip SV modeli ile birlikte sıçrama bileşenli modeller, oynaklık-ortalama etkileşimini içeren modeller, hareketli ortalama yenilikleri barındıran modeller, t-dağılımına sahip yenilik içeren modeller ve kaldıraç etkisini dikkate alan modeller yer almaktadır. Ayrıca, GARCH(2,1) ve ikinci dereceden otoregresif log-oynaklık sürecine sahip SV modeli de çalışmaya dahil edilmiştir.

Bu tezde, söz konusu oynaklık modellerinin başarımları, kestirim doğruluğu ve tahmin gücü olmak üzere iki temel başlık altında değerlendirilmiştir.

Kestirim aşamasında, modellerin günlük getiriler üzerindeki uyumu Bayesçi yöntemle ölçülmüş; her modelin log-marjinal olasılığı hesaplanmış ve model parametrelerinin artıkküçük ortalamaları elde edilmiştir. Sonuçlara göre, her iki kripto para birimi için

en başarılı model SV-t olup, genel olarak SV modelleri GARCH modellerine kıyasla üstün performans sergilemektedir. GARCH-t ikinci sırada yer almakta, bu durum t-dağılımının katkısını göstermektedir. Sıçrama bileşeni hem Bitcoin hem de Ethereum için GARCH modelinin başarımını artırırken, Ethereum'un SV modelinde belirgin bir etki oluşturmamaktadır. Bitcoin'de AR(2) yapısı, AR(1)'e göre daha zayıf sonuç verirken, Ethereum'da AR(2) yapısı daha başarılı olmuştur. Hareketli ortalama bileşeni Ethereum'un SV modeli için olumlu katkı sağlamıştır. Ortalama üzerindeki oynaklık etkisi modellerde anlamlı bulunmamıştır. Kaldıraç etkisi GARCH modeli için faydalı olurken, SV modellerinde anlamlı değildir. Ethereum için kaldıraç etkisi parametresi de anlamlı bulunmamıştır.

Tahmin başarımını değerlendirmek üzere log-tahmin skoru kullanılmıştır. Elde edilen bulgular, kripto paralara göre farklılık göstermektedir: Bitcoin için GARCH-t modeli en iyi sonuçları verirken, Ethereum için en başarılı model GARCH-J olmuştur. AR(2) yapısı yalnızca Bitcoin için SV modelinin tahmin gücünü artırmıştır. Sıçrama bileşeni, hem GARCH hem de SV modellerinin Bitcoin tahmin gücünü artırırken, Ethereum için yalnızca GARCH modeline anlamlı katkı sunmuştur. Oynaklık-ortalama etkileşimi Bitcoin için anlamlı bulunmuş, Ethereum için gerekli görülmemiştir. Hareketli ortalama bileşeni, Bitcoin'in SV modeli için tahmin başarımını iyileştirirken, diğer modellerde sınırlı katkı sağlamıştır. t-dağılımı genel olarak tahmin başarımını artırmıştır. Kaldıraç etkisi Bitcoin için faydalı bulunmuş, Ethereum için anlamlı bir katkı sağlamamıştır.

1. INTRODUCTION

In recent years, cryptocurrencies have attracted significant attention from academics, investors, policymakers, and media outlets. Defined as digital assets primarily designed for use as a medium of exchange secured by cryptographic methods (Nakamoto, 2008), cryptocurrencies are often regarded as high-risk and highly volatile, operating within uncertain regulatory frameworks. Nonetheless, they function both as exchange mediums and speculative assets, frequently offering returns that surpass those of traditional financial markets (Nica et al., 2022). Volatility remains a central theme in finance, playing a critical role for investors, risk managers, and regulators alike. Given their speculative nature, intense trading activity, and media coverage, cryptocurrencies have become prominent subjects of volatility research. This thesis seeks to deepen the understanding and modeling of volatility in major cryptocurrencies, specifically Bitcoin and Ethereum.

Among time-varying volatility models, the Generalized Autoregressive Conditional Heteroskedasticity (GARCH) framework is one of the most established. In GARCH models, conditional variance is expressed as a deterministic function of historical data. Conversely, Stochastic Volatility (SV) models treat volatility as an unobservable variable governed by its own stochastic process, fundamentally distinguishing them from GARCH approaches. These two model families are non-nested and offer distinct methods for capturing the dynamics of time-varying volatility.

Although GARCH and SV models have been widely employed to estimate and forecast asset price volatility—particularly in equity (Endri et al., 2021), (Aliyev et al., 2020), (Qu and Perron, 2013) and energy markets (Chan and Grant, 2016)—their comparative use in cryptocurrency markets remains underexplored (Tiwari et al., 2019). In particular, few studies have jointly evaluated these models regarding both estimation accuracy and predictive performance for cryptocurrency volatility. This

this thesis addresses this gap by applying GARCH and SV models to Bitcoin and Ethereum and comparing their performance.

The analysis focuses on Bitcoin and Ethereum, the two largest cryptocurrencies by market capitalization, and employs two main volatility modeling frameworks: GARCH-type models and SV-type models. Specifically, seven GARCH models and their SV counterparts are examined, following the formulations in (Chan and Grant, 2016). The GARCH models include: (1) the standard GARCH(1,1); (2) GARCH(2,1) (GARCH-2); (3) GARCH with jump components (GARCH-J); (4) GARCH-in-mean (GARCH-M); (5) GARCH with moving average innovations (GARCH-MA); (6) GARCH with t -distributed innovations (GARCH- t); and (7) GARCH with asymmetric leverage effects (GARCH-GJR). The SV models analyzed include: the baseline SV model with AR(1) log-volatility; an AR(2) extension (SV-2); a version incorporating jumps (SV-J); a volatility-in-mean variant (SV-M); a version with moving average terms (SV-MA); a heavy-tailed variant with t -distributed shocks (SV- t); and an SV model accounting for leverage effects (SV-L), where negative returns disproportionately increase volatility.

The objective of this thesis is to investigate Bitcoin and Ethereum volatility through two main lenses. First, the models' fit to daily return data is assessed. Using Bayesian techniques, we compute each model's log marginal likelihood and estimate posterior parameter means. The marginal likelihood represents the integrated probability of the observed data over the parameter space, weighted by the prior distributions. A higher marginal likelihood suggests the model provides a better explanation of the observed data. Second, we evaluate forecasting performance using the log-predictive score for each model with respect to Bitcoin and Ethereum returns.

The key findings can be summarized as follows: First, in terms of estimation, the SV- t model achieves the highest marginal likelihood for both Bitcoin and Ethereum. Except for the GARCH-J model, all SV models outperform their GARCH counterparts in estimating Bitcoin returns, suggesting superior robustness to model misspecification and abrupt changes, consistent with (Yu, 2002) and (Chan and Grant, 2016). Second, the GARCH- t model consistently ranks second, highlighting the benefits of

t -distributed innovations. Third, an AR(1) specification performs better for Bitcoin, while an AR(2) process improves results for Ethereum. Fourth, jump components enhance estimation performance in both GARCH and SV models for Bitcoin, but have limited impact on Ethereum's SV models, consistent with Tiwari et al. (2019). Fifth, volatility-in-mean effects offer minimal contribution to estimation accuracy. Sixth, moving average innovations are generally insignificant for Bitcoin but enhance Ethereum's SV model. Seventh, the leverage effect improves the GARCH-GJR model for Bitcoin but remains irrelevant in SV models and for Ethereum.

Regarding forecasting, the results show: First, the GARCH-t model delivers the best performance for Bitcoin, while GARCH-J leads for Ethereum. Second, AR(2) terms do not improve GARCH forecasts for Bitcoin or SV forecasts for Ethereum, though they significantly benefit Bitcoin SV models. Third, jump components notably improve Bitcoin forecasts and enhance Ethereum's GARCH predictions, with slight gains in SV models. Fourth, volatility-in-mean terms improve Bitcoin forecasts but are redundant for Ethereum. Fifth, moving average innovations improve Bitcoin SV forecasts and marginally benefit both GARCH and SV models for Ethereum. Sixth, t -distributed innovations strengthen forecasts across models. Seventh, the leverage effect improves Bitcoin's SV-L forecasts and modestly benefits the GARCH-GJR model, but is insignificant for Ethereum.

The remainder of this thesis is structured as follows. Chapter 2 provides an overview of the cryptocurrency market, detailing its structure and fundamental principles, including a classification of cryptocurrencies such as payment tokens, utility tokens, stablecoins, and central bank digital currencies (CBDCs), as well as an examination of supply and demand dynamics. Chapter 3 presents a comprehensive review of the existing literature on cryptocurrency volatility. Chapter 4 outlines the empirical analysis, describing the data, the employed GARCH and Stochastic Volatility models, and the Bayesian estimation methodology, including details on the Gibbs sampler, prior distributions, and model comparison. Chapter 5 reports the forecasting results, comparing the predictive performance of the models. Finally, Chapter 6 summarizes the key findings of the thesis and offers concluding remarks and suggestions for future research.

2. CRYPTO MARKET STRUCTURE AND FUNDAMENTALS OF CRYPTOCURRENCIES

This chapter offers a comprehensive review of the cryptocurrency market and explains essential concepts. Cryptocurrencies are digital assets secured through cryptographic methods, including public-private key infrastructure, elliptic curve cryptography, and hashing algorithms, which guarantee transaction security. These technologies allow users to send payments directly online without third-party intermediaries (Nakamoto, 2008), (Kube, 2018).

The origins of cryptocurrencies date back to the 1980s. In 1983, cryptographer David Chaum introduced ecash, a form of digital money protected by cryptographic principles (Chaum, 1983). Later, in 1995, Chaum proposed Digicash, an early digital payment tool that enabled users to withdraw funds and assign encrypted keys, ensuring privacy from third-party tracking (Chaum et al., 1990).

In 1996, the NSA released the paper “How to Make a Mint: The Cryptography of Anonymous Electronic Cash” (Law et al., 1996), outlining a conceptual framework for anonymous digital currency. Soon after, Wei Dai introduced b-money (Dai, 1998), and Nick Szabo proposed Bit Gold (Peck, 2012), an electronic currency system requiring Proof-of-Work—setting the stage for Bitcoin.

The 2008 global financial crisis, often called the worst since the Great Depression, sparked public demand for alternatives to centralized banking. The collapse of major institutions like Lehman Brothers highlighted flaws in the financial system, leading to interest in decentralized solutions.

In October 2008, under the pseudonym Satoshi Nakamoto, Bitcoin was introduced (Nakamoto, 2008). The proposed system allowed peer-to-peer exchanges secured with cryptography, eliminating the need for trusted intermediaries. Bitcoin’s blockchain network launched on January 3, 2009, operating as a distributed ledger upheld by miners verifying transactions worldwide.

Following Bitcoin, projects like Namecoin and Litecoin (2011), Peercoin (2012), and Ethereum (2013, proposed by Vitalik Buterin and colleagues) expanded the ecosystem. Ethereum, launched in 2015, introduced programmable smart contracts, driving innovation in decentralized applications.

A core feature of cryptocurrencies is decentralization, reducing dependence on governments or central entities. While most use decentralized blockchains, some (e.g., Ripple) operate on alternative architectures (Nica et al., 2022). Blockchain ensures secure recordkeeping through consensus among distributed nodes.

Cryptocurrencies offer privacy, access to global markets, portfolio diversification, and low inflation risk via capped supplies. Yet, they also present challenges: limited user knowledge, absence of institutional backing, restricted merchant adoption, potential misuse in illegal activities, extreme volatility, and systemic risks (Rice, 2019).

2.1 Types of Cryptocurrencies

2.1.1 Payment Cryptocurrencies

Payment-focused cryptocurrencies act as digital money, often operating on dedicated blockchains without smart contract features. Many have fixed supplies, contributing to deflationary tendencies. Notable examples include Bitcoin, Litecoin, Monero, Dogecoin, and Bitcoin Cash.

Among them, meme coins stand out—altcoins inspired by internet humor or trends. Dogecoin, Shiba Inu, and Pepe lead the meme coin market, representing around 67% of total meme coin capitalization (Cog). Although they offer potential short-term gains, meme coins are often highly speculative, driven by social media and influencer buzz, with elevated risks of scams or loss of interest.

Early cryptocurrencies, such as Bitcoin and Litecoin, rely on Proof-of-Work (PoW) consensus, where miners solve computational puzzles to validate transactions. However, not all cryptocurrencies require mining, and some use alternative mechanisms.

2.1.2 Utility Tokens

Utility tokens, typically issued on existing blockchains, provide access to services or features, often launched via Initial Coin Offerings (ICOs). Ethereum (Buterin et al., 2013) pioneered smart contract capabilities, enabling decentralized applications (DApps). Utility tokens can be inflationary and cover categories like service tokens (e.g., Storj), governance tokens (e.g., MKR), exchange tokens (e.g., BNB, KCS), media tokens (e.g., BAT), and non-fungible tokens (NFTs) used in art and gaming.

Proof-of-Stake (PoS), employed by platforms like Ethereum, selects validators based on staked assets rather than computational power. For instance, operating an Ethereum validator node requires staking 32 ETH. PoS reduces energy use significantly, cutting Ethereum's carbon footprint by over 99% after its transition (Dig).

2.1.3 Stablecoins

Stablecoins aim to maintain price stability, usually pegged to fiat currencies like the US dollar and backed by reserves. Popular examples include Tether (USDT). Despite their intended stability, failures like TerraUSD's collapse in 2022 reveal inherent risks.

2.1.4 Central Bank Digital Currencies (CBDCs)

CBDCs are government-issued digital currencies, contrasting with decentralized crypto assets. While they can incorporate blockchain for efficiency, they prioritize regulatory oversight and user identification. Countries including China, India, and members of the EU are exploring or piloting CBDCs, focusing on financial inclusion, cross-border payments, and public trust (CEB).

CBDCs divide into wholesale (institutional use) and retail (public use) forms. While promising, they raise privacy and data protection concerns, such as safeguarding personal information, preventing re-identification, and complying with international data transfer regulations.

2.2 Cryptocurrencies Supply and Demand Dynamics

As of March 2025, CoinMarketCap (Coi) tracks 13,240 cryptocurrencies and 819 exchanges, with a total market cap near \$2.67 trillion and a daily trading volume of \$43.65 billion. Bitcoin trades at approximately \$83,053, and Ethereum at \$1,789, holding 62% and 8.1% market dominance, respectively. On Ethereum, transaction fees average 0.91 Gwei (10^{-9} ETH).

Bitcoin's value derives from capped supply (21 million coins), halving cycles reducing mining rewards every four years, and sensitivity to regulatory and media events. The last halving in April 2024 reduced rewards to 3.125 BTC per block.

Around 19.84 million Bitcoins are currently in circulation, with mining serving as the issuance method. Miners secure the network by solving PoW puzzles, earning transaction fees and block rewards. Mining ensures decentralization and prevents double-spending but raises environmental concerns due to high energy consumption.

Bitcoin demand grows via investment interest, adoption in inflation-hit regions, and speculation. Notable price surges occurred in 2017, 2021, and 2024, driven by factors like U.S. ETF approvals and SEC decisions. For example, Bitcoin hit \$69,000 post-ETF approval in 2021 but fell back amid regulatory and geopolitical pressures.

Altcoins—non-Bitcoin cryptocurrencies—include Ethereum, which powers smart contracts, DApps, and NFTs. Unlike Bitcoin's capped supply, Ethereum currently circulates 120.65 million ETH. Bitcoin's dominance fluctuated from 80% in 2017 to 57% in late 2024, with Ethereum, Tether, Binance Coin, and Solana among top competitors.

3. LITERATURE REVIEW

This section presents a summarized and paraphrased review of the key literature relevant to this thesis.

Katsiampa (2017) explored Bitcoin volatility by applying six variations of the GARCH model, integrating an AR term into the mean equation alongside first-order GARCH specifications for variance. Analyzing over 2,200 daily observations, the study evaluated model performance using AIC, BIC, HQ, and log-likelihood metrics, ultimately identifying the AR-CGARCH model as superior due to its ability to capture both short-term and long-term volatility dynamics. The findings underline the suitability of component models for cryptocurrencies, which often exhibit persistent and nonlinear volatility patterns.

Kim et al. (2021) examined the volatility of nine prominent cryptocurrencies using both GARCH and Stochastic Volatility (SV) models. The analysis, spanning low- and high-volatility periods, applied models such as GARCH(1,1), TGARCH, IGARCH, and SV with normal innovations. Forecast accuracy, assessed through logarithmic Mean Squared Prediction Error (MSE), highlighted the SV model's consistent outperformance, especially over longer forecasting horizons. Principal Component Analysis (PCA) further revealed common volatility trends among assets.

Trucíos (2019) assessed Bitcoin's volatility forecasting by comparing robust and non-robust GARCH-type models across various error distributions, including Normal, Student-t, GED, and NIG. Utilizing realized variance measures and loss functions like QLIKE and MSE, the study found that models like TGARCH, AVGARCH, CGARCH, IGARCH, and particularly Robust GARCH delivered superior predictive accuracy, emphasizing the value of robust techniques for volatility and risk estimation.

Catania et al. (2018) focused on forecasting volatility for Bitcoin, Ethereum, Ripple, and Litecoin using standard GARCH and several extensions of the Score-Driven

GHSKT model. They evaluated models over different forecast horizons and found that incorporating leverage, time-varying skewness, and fractional integration generally enhanced performance, especially for Litecoin and Ripple. The Score-Driven models surpassed standard GARCH, with gains amplifying over longer periods.

Dyhrberg (2016) investigated whether Bitcoin behaves more like a commodity or currency by integrating macro-financial variables into GARCH-based models. The study showed Bitcoin exhibiting characteristics of both gold and fiat currencies, with significant volatility persistence and symmetric shock responses, suggesting its dual nature and potential applications in portfolio diversification.

Balcilar et al. (2017) analyzed the predictive relationship between Bitcoin trading volume and its returns and volatility using a non-parametric causality-in-quantiles approach. Results indicated that volume predicts returns during stable market conditions but offers limited insights into volatility across different market regimes.

Hattori (2020) compared various GARCH-family models in forecasting Bitcoin's realized volatility, computed from intraday data. Models accounting for asymmetry, such as APARCH and EGARCH, outperformed others, particularly when paired with normal distribution assumptions. These results emphasize the importance of asymmetric effects and distributional choices in volatility modeling.

Fakhfekh and Jeribi (2020) evaluated 16 cryptocurrencies using multiple GARCH-family models and error distributions. The study found that TGARCH and EGARCH models, especially under double-exponential or generalized error assumptions, most effectively captured cryptocurrency-specific volatility, which responds more strongly to positive shocks—a deviation from traditional financial assets.

Caporale and Zekokh (2019) applied Markov-switching and standard GARCH-type models to four major cryptocurrencies, using rolling-window Value at Risk (VaR) and Expected Shortfall (ES) forecasts. The analysis revealed that regime-switching models generally outperformed single-regime alternatives, with model performance varying across cryptocurrencies and regimes.

Chaim and Laurini (2018) used log-stochastic volatility models with and without jumps, estimating parameters via Bayesian MCMC methods. Findings underscored the importance of accounting for jumps to accurately model Bitcoin's volatility, highlighting that volatility jumps have lasting effects, whereas return jumps exert short-lived impacts.

Baur and Dimpfl (2018) examined asymmetric volatility across the largest cryptocurrencies using TGARCH and Quantile Autoregressive models. The study identified a pronounced asymmetric response to positive news, attributed to behavioral factors like FOMO and market manipulation, differentiating crypto markets from traditional ones.

Cheikh et al. (2020) introduced the Smooth Transition GARCH (ST-GARCH) model, comparing it to other GARCH-family models across four major cryptocurrencies. The ST-GARCH model provided superior fit, especially in capturing asymmetric effects, with Ethereum being the only case where a ZGARCH model performed slightly better.

Guo (2022) analyzed Bitcoin futures' volatility using multiple GARCH variations under different distributional assumptions. Their results consistently favored the GARCH-NIG specification, which delivered the best fit and Value at Risk forecasts, suggesting it as a robust choice for futures markets.

Bergsli et al. (2022) compared GARCH and Heterogeneous Autoregressive (HAR) models, employing realized variance from high-frequency Bitcoin data. HAR models generally outperformed GARCH variants, though in turbulent or longer-horizon scenarios, models like EGARCH proved competitive.

Chan and Grant (2016) and Tiwari et al. (2019) extended the comparison of GARCH and SV models to commodities and cryptocurrencies, respectively. Both studies, using Bayesian estimation techniques, concluded that SV models consistently outperform GARCH counterparts, particularly when incorporating heavy-tailed distributions. These results reinforce the broader applicability and superiority of SV approaches in modeling financial volatility.

Overall, the literature highlights the evolving sophistication of volatility models applied to cryptocurrencies, emphasizing the importance of model flexibility,

distributional assumptions, and asymmetry in capturing the unique dynamics of digital assets.



4. EMPIRICAL RESULTS

4.1 Data

In this thesis, we use the package "cryptoQuotes: Open Access to Cryptocurrency Market Data, Sentiment Indicators and Interactive Charts" (Korkmaz, 2024) to obtain daily Bitcoin and Ethereum cryptocurrency data. The cryptoQuotes package provides market data, sentiment indicators, and interactive charting tools for investors and researchers. Using this R package, it is easy to acquire open, high, low, and close (OHLC) prices for cryptocurrencies at frequencies ranging from seconds to months, across major cryptocurrency exchanges such as Binance and KuCoin (Gu et al., 2022). Cryptocurrency exchanges enable users to trade digital currencies for traditional fiat money or swap one cryptocurrency for another. KuCoin, crypto exchange founded in 2017, is one of the most popular cryptocurrency exchanges in the world, with a daily trading volume exceeding millions of dollars.

This study focuses on the daily closing prices of Bitcoin and Ethereum, obtained from the KuCoin exchange for the period between October 19, 2017, 03:00 and February 28, 2025, 03:00. The dataset for each cryptocurrency consists of 2,683 observations.

Figure 4.1 and Figure 4.2 demonstrates the time series plots of Bitcoin and Ethereum, respectively. Figure 4.1 shows that in 2017, Bitcoin's price increased, followed by a decline in 2018. Between 2018 and 2019, it experienced a recovery period with an upward trend. Toward the end of 2020, the price surged significantly. From the pandemic-spike year of 2020 to 2022, the price continued to rise, reaching an all-time high of \$64,800 in 2021. However, between 2022 and 2024, the price declined. After 2024, following the approval of Bitcoin ETFs, the price rose again but experienced a slight decrease at the beginning of 2025.

Figure 4.2 illustrates that Ethereum reached its all-time high of \$1,433 in early 2018, then declined to around \$130 by the end of that year. Between 2019 and 2020, it

recovered, reaching approximately \$750. In 2021, Ethereum experienced a major surge and hit a new all-time high of \$4,865. Between 2021 and 2022, its price decreased considerably. Toward the end of 2024, its price increased again following ETF approvals. However, in 2025, the price declined once more.

The descriptive statistics for Bitcoin and Ethereum are presented in the Table 4.1.

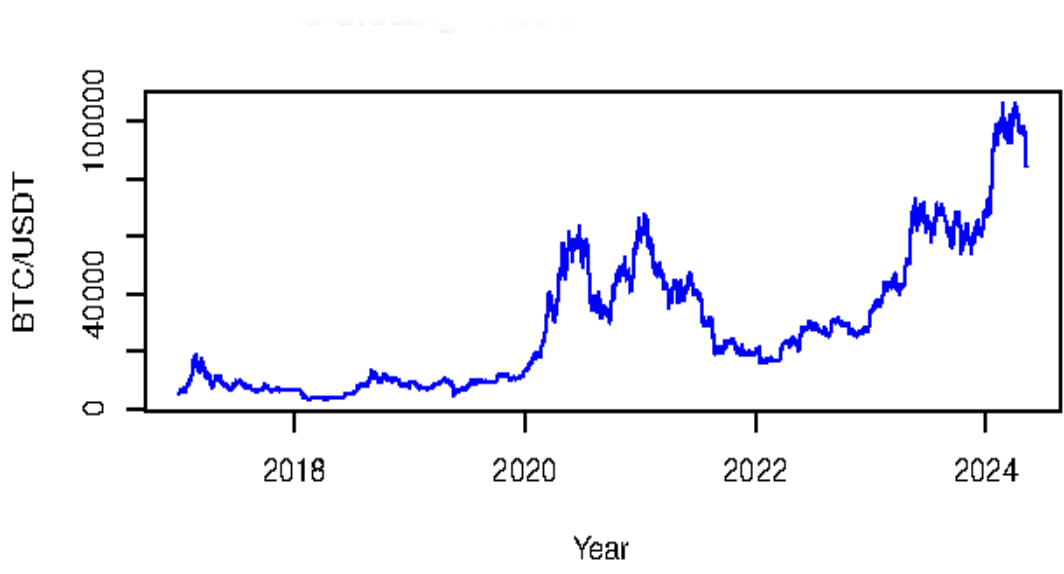


Figure 4.1: Bitcoin Daily Closure Prices.

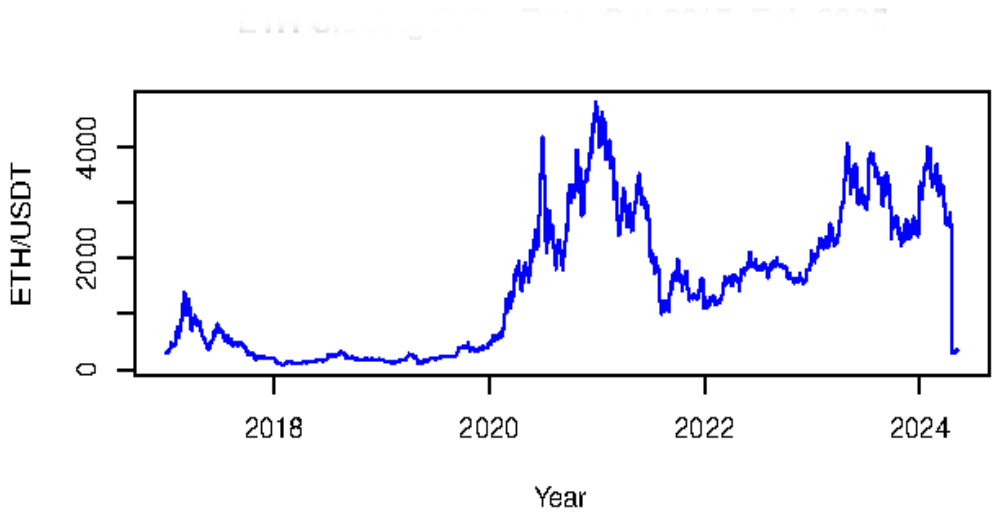


Figure 4.2: Ethereum Daily Closure Prices.

Table 4.1: Statistical Summary of Bitcoin and Ethereum Daily Close Prices.

	Bitcoin	Ethereum
Total Sample Size	2683	2683
Mean	29164.05	1517.49
Std. Deviation	24113.52	1235.27
Skewness	1.08	0.5
Kurtosis Above Normal	0.54	-0.94

Table 4.1 shows that both Bitcoin and Ethereum data are right-skewed, as their skewness values are greater than zero. In terms of excess kurtosis, Bitcoin data is leptokurtic, indicating a heavy-tailed distribution, since its excess kurtosis value exceeds zero. This implies a higher probability of observing extreme values in Bitcoin returns compared to a normal distribution. In contrast, Ethereum data is platykurtic, with a negative excess kurtosis value, suggesting a light-tailed distribution. This means that extreme values are less likely in Ethereum returns compared to the normal distribution. Moreover, the standard deviation of Bitcoin is higher than that of Ethereum, indicating that Bitcoin exhibits greater volatility.

In this study, all models are implemented using the log returns of the daily closing prices of Bitcoin and Ethereum obtained from the KuCoin cryptocurrency exchange. The log returns are defined as follows:

$$y_t = 100 * \log(P_t/P_{t-1}), \quad t = 2, 3, 4 \dots 2683 \quad (4.1)$$

Here, y_t denotes the daily log return at time t and P_t represents the closing cryptocurrency prices of Bitcoin and Ethereum in Kucoin crypto exchange.

To examine the volatility characteristics of daily Bitcoin and Ethereum data, we begin by defining volatility clustering. Volatility clustering refers to the phenomenon where large changes in asset prices tend to be followed by large changes (of either sign), and small changes tend to be followed by small changes. Our analysis covers three categories of figures: returns, squared forms, and absolute values. Additionally, we plot their correlograms—specifically, the Sample Autocorrelation Function (ACF)-to detect the presence of volatility clustering.

Figure 4.3, Figure 4.5 and Figure 4.7 depicts the daily return graph, return squares and absolute return graphs of Bitcoin, separately. In the return graph of Bitcoin, as

indicated in Figure 4.3, it is observed that periods of high volatility are often followed by further high volatility, and periods of low volatility tend to be followed by low volatility. For example, for the first 80 observations, large volatility is followed by further large movements. Conversely, between the 2100th and 2150th observations, periods of low volatility persist. The correlogram of Bitcoin returns shows no significant autocorrelation in Figure 4.4, indicating a lack of linear dependence in returns. However, the correlograms of squared returns in Figure 4.6 and absolute returns in Figure 4.8 reveal significant autocorrelations at various lags, confirming the presence of volatility clustering in Bitcoin data.

Figure 4.9, Figure 4.11 and Figure 4.13 illustrates the daily return graph, return squares and absolute return graphs of Ethereum, respectively. Similarly, in the return graph of Ethereum, as shown in Figure 4.9, nearly all periods of high volatility tend to be followed by high volatility. While the correlogram of Ethereum returns in Figure 4.10 does not exhibit significant autocorrelation, the correlograms of squared in Figure 4.12 and absolute returns in Figure 4.14 show clear evidence of autocorrelation across multiple lags. This again suggests the presence of volatility clustering. To avoid convergence problems in the estimation process, we omit 35 extreme log return values for Ethereum that are either less than -15 or greater than 15.

4.2 Models

In this section, we focus on seven GARCH models and seven SV models to analyze the volatility of Bitcoin and Ethereum. GARCH models were developed by (Bollerslev, 1986) and SV models were proposed by (Taylor, 1994). Detailed explanations of these models can be found in the textbooks by (Francq and Zakoian, 2019) and (Martin et al., 2013).

4.2.1 GARCH Models

The first model considered is the standard GARCH(1,1) model. Equation 4.2 presents the constant mean specification, and Equation 4.3 represents the innovation term of the

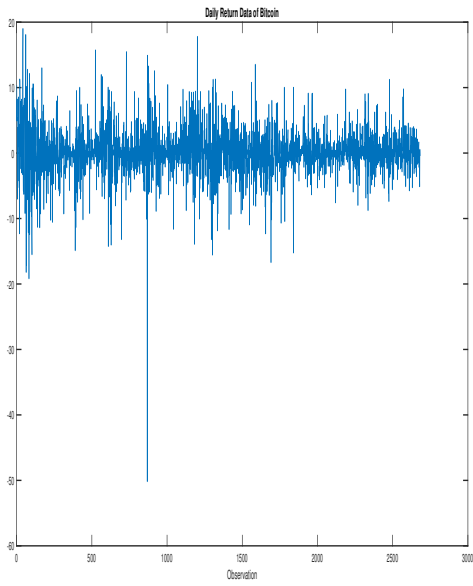


Figure 4.3: The Daily Return Graph of Bitcoin.

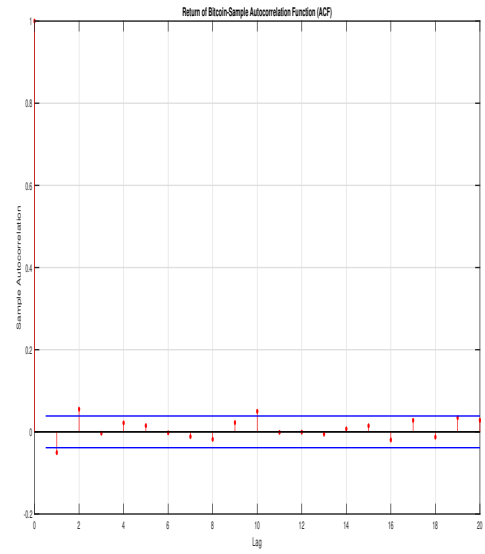


Figure 4.4: The Correlogram of Daily Return of Bitcoin.

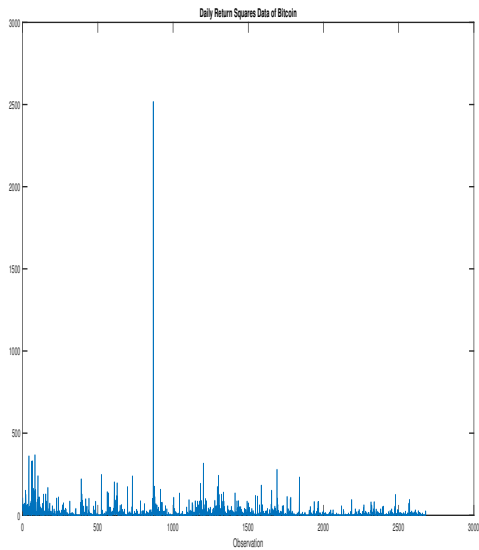


Figure 4.5: The Daily Return Squares Graph of Bitcoin.

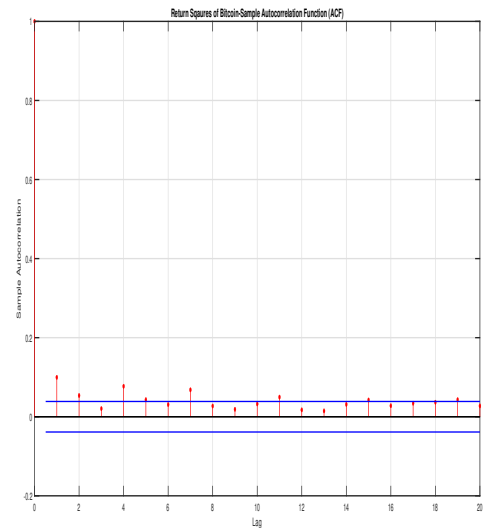


Figure 4.6: The Correlogram of Daily Return Squares of Bitcoin.

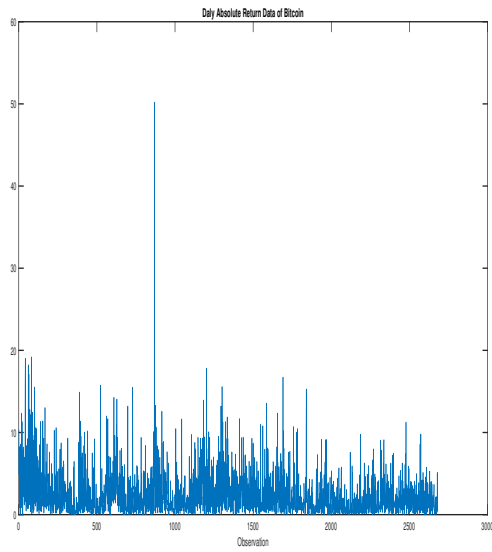


Figure 4.7: The Daily Absolute Return Graph of Bitcoin.

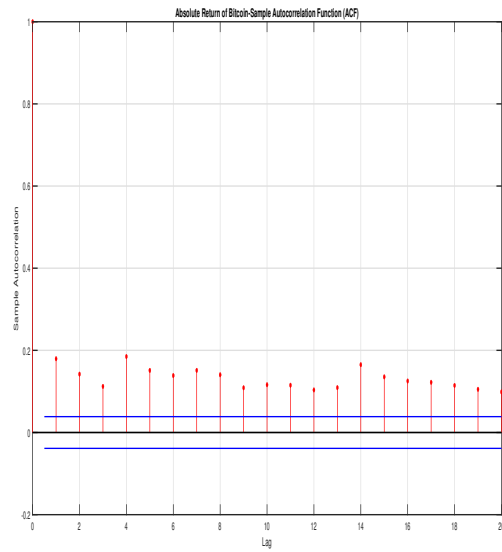


Figure 4.8: The Correlogram of Daily Absolute Return of Bitcoin.

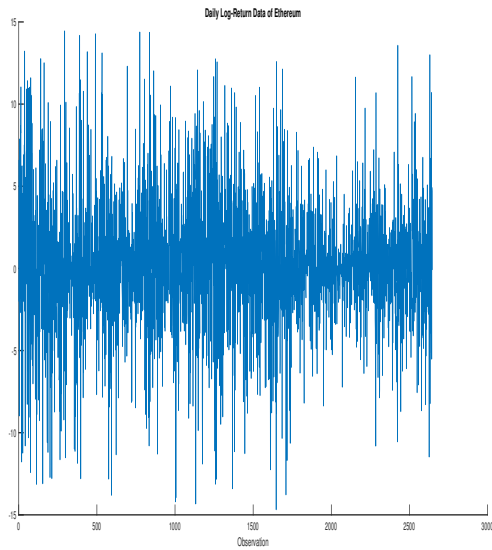


Figure 4.9: The Daily Return Graph of Ethereum.

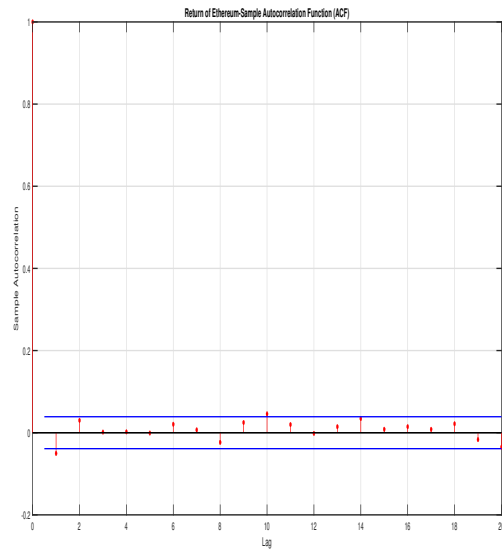


Figure 4.10: The Correlogram of Daily Return of Ethereum.

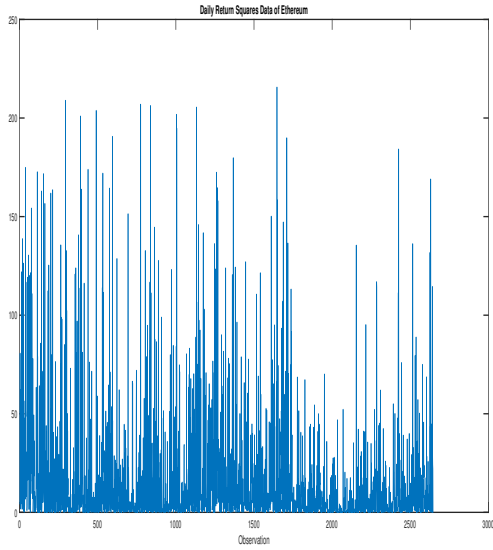


Figure 4.11: The Daily Return Squares Graph of Ethereum.

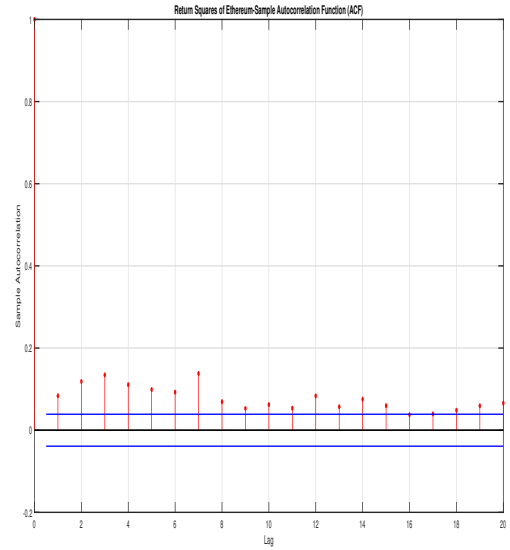


Figure 4.12: The Correlogram of Daily Return Squares of Ethereum.

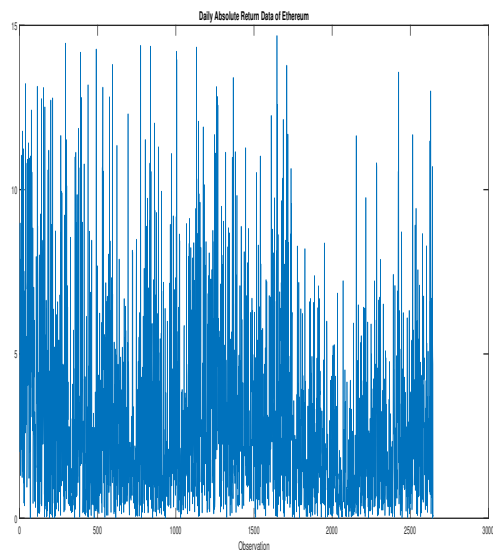


Figure 4.13: The Daily Absolute Return Graph of Ethereum.

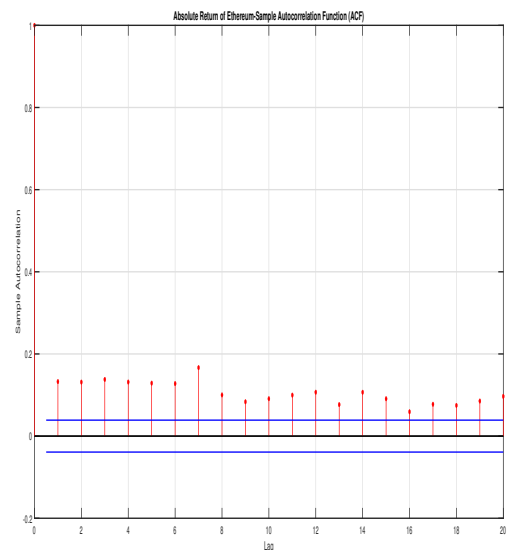


Figure 4.14: The Correlogram of Absolute Return of Ethereum.

standard GARCH(1,1) model.

$$y_t = \mu + \varepsilon_t, \quad \varepsilon_t \sim \mathcal{N}(0, \sigma_t^2), \quad (4.2)$$

$$\varepsilon_t = \sigma_t * z_t, \quad z_t \sim \mathcal{N}(0, 1), \quad (4.3)$$

where y_t represents the return at time t , μ is the mean return and ε_t are independent innovation terms (or the error terms). Note that we also express ε_t as $\varepsilon_t = \sigma_t * z_t$, where $z_t \sim N(0, 1)$ and σ_t is the conditional standard deviation and is called volatility.

The conditional variance equation of GARCH (1,1) is defined as follows:

$$\sigma_t^2 = \alpha_0 + \alpha_1 \varepsilon_{t-1}^2 + \beta_1 \sigma_{t-1}^2, \quad (4.4)$$

where σ_t^2 is the conditional variance at time t , α_0 represents the base level of volatility, α_1 determines how shocks to returns affect the future volatility, and β_1 reflects the persistence of past volatility. For the initial values, we assume that, σ_0^2 is constant and $\varepsilon_0 = 0$. To always ensure the stationarity and positivity of σ_t^2 , the parameters must satisfy $\alpha_0 > 0$, $\alpha_1 \geq 0$, $\beta_1 \geq 0$ and $\alpha_1 + \beta_1 < 1$. The conditional variance process σ_t^2 (4.4), is a deterministic function of the model parameters and past data and follows AR(1) process.

The second model, GARCH(2,1), denoted as GARCH-2, extends the GARCH(1,1) model by allowing second-order autoregression in volatility:

$$y_t = \mu + \varepsilon_t, \quad \varepsilon_t \sim \mathcal{N}(0, \sigma_t^2), \quad (4.5)$$

$$\sigma_t^2 = \alpha_0 + \alpha_1 \varepsilon_{t-1}^2 + \beta_1 \sigma_{t-1}^2 + \beta_2 \sigma_{t-2}^2. \quad (4.6)$$

As in GARCH(1,1), for the initial values, we assume that σ_0^2 is constant and $\varepsilon_0 = \varepsilon_{-1} = 0$. The conditions $\alpha_0 > 0$, $\alpha_1 > 0$, $\beta_1 > 0$, $\beta_2 > 0$, and $\alpha_1 + \beta_1 + \beta_2 < 1$ must be satisfied to ensure the positivity and stationarity of the variance process σ_t^2 .

The third model, GARCH with jumps (GARCH-J), incorporates infrequent ‘‘jumps’’ in the mean equation:

$$y_t = \mu + k_t q_t + \varepsilon_t, \quad \varepsilon_t \sim \mathcal{N}(0, \sigma_t^2), \quad (4.7)$$

$$\sigma_t^2 = \alpha_0 + \alpha_1 (y_{t-1} - \mu)^2 + \beta_1 \sigma_{t-1}^2, \quad (4.8)$$

where the jump variable $q_t \in \{0, 1\}$ and its success probability is $P(q_t = 1) = \kappa$. Thus, $q_t = 1$ implies that a jump takes place at time t and its size is determined by k_t , which is defined as $k_t \sim \mathcal{N}(\mu_k, \sigma_k^2)$. Here, κ , μ_k and σ_k^2 are additional parameters that we need to estimate.

The fourth model, GARCH-in-Mean (GARCH-M), introduced by (Engle et al., 1987) and employed in studies such as (Elyasiani and Mansur, 1998) and (Mouna and Anis, 2016), integrates the conditional variance directly into the mean equation.

$$y_t = \mu + \lambda \sigma_t^2 + \varepsilon_t, \quad \varepsilon_t \sim \mathcal{N}(0, \sigma_t^2), \quad (4.9)$$

$$\sigma_t^2 = \alpha_0 + \alpha_1 (y_{t-1} - \mu - \lambda \sigma_{t-1}^2)^2 + \beta_1 \sigma_{t-1}^2. \quad (4.10)$$

If $\lambda = 0$, the GARCH-M model reduces to the standard GARCH model. This parameter shows the effect of conditional variance on the returns. Adding σ_t^2 in the mean equation captures volatility feedback.

The fifth model, GARCH-MA, integrates a first-order Moving Average (MA(1)) process into the innovations:

$$y_t = \mu_t + \varepsilon_t, \quad (4.11)$$

$$\varepsilon_t = u_t + \psi u_{t-1}, \quad u_t \sim \mathcal{N}(0, \sigma_t^2), \quad (4.12)$$

$$\sigma_t^2 = \alpha_0 + \alpha_1 \varepsilon_{t-1}^2 + \beta_1 \sigma_{t-1}^2. \quad (4.13)$$

For the MA parameter ψ , we assume that $|\psi| < 1$ to ensure invertibility. This model captures short-term correlation in the return series. This model captures the return series to be correlated over time and might be better in terms of the short-run dynamics of the series.

The sixth model, GARCH-t, assumes Student's t distribution for the innovation terms:

$$y_t = \mu_t + \varepsilon_t \quad \varepsilon_t \sim t_\nu(0, \sigma_t^2), \quad (4.14)$$

$$\sigma_t^2 = \alpha_0 + \alpha_1 \varepsilon_{t-1}^2 + \beta_1 \sigma_{t-1}^2, \quad (4.15)$$

where the conditional variance σ_t^2 formula is the same as (4.4). $t_\nu(0, \sigma_t^2)$ denotes the Student's t distribution with zero mean, σ_t^2 conditional variance and ν degrees of freedom. The heavy tails of the t -distribution allow for more extreme return values compared to the normal distribution.

The seventh model, GARCH-GJR, developed by (Glosten et al., 1993), introduces asymmetry in response to negative shocks:

$$y_t = \mu + \varepsilon_t, \quad \varepsilon_t \sim \mathcal{N}(0, \sigma_t^2), \quad (4.16)$$

$$\sigma_t^2 = \alpha_0 + (\alpha_1 + \delta_1 \mathbb{I}(\varepsilon_{t-1} < 0)) \varepsilon_{t-1}^2 + \beta_1 \sigma_{t-1}^2, \quad (4.17)$$

where $\mathbb{I}(\cdot)$ demonstrates the indicator function. The asymmetric leverage effect is determined by the parameter δ_1 . GARCH-GJR model enables the potentially larger impact of negative excess returns on the conditional variance.

4.2.2 Stochastic Volatility Models

In this section, we describe the SV models used in this thesis. Unlike GARCH models, where conditional variance is a deterministic function of past data and parameters, SV models treat volatility as a latent random variable.

The first stochastic volatility model considered is the standard stochastic volatility (SV) model:

$$y_t = \mu + \varepsilon_t^y, \quad \varepsilon_t^y \sim \mathcal{N}(0, e_t^h), \quad (4.18)$$

$$h_t = \mu_h + \phi_h(h_{t-1} - \mu_h) + \varepsilon_t^h, \quad \varepsilon_t^h \sim \mathcal{N}(0, w_h^2), \quad (4.19)$$

where h_t denotes the log-volatility, which follows a stationary AR(1) process with $|\phi_h| < 1$, μ_h represents the unconditional mean, and w_h^2 is the variance of the innovation term in the log-volatility equation. We assume that ε_t^y and ε_t^h are independently distributed. Moreover, $h_1 \sim \mathcal{N}(\mu_h, w_h^2/(1 - \phi_h^2))$ shows the initialization of the process.

The SV-2 model extends the standard SV model by assuming that log-volatility follows an AR(2) process:

$$y_t = \mu + \varepsilon_t^y, \quad \varepsilon_t^y \sim \mathcal{N}(0, \mathbf{e}_t^h), \quad (4.20)$$

$$h_t = \mu_h + \phi_h(h_{t-1} - \mu_h) + \rho_h(h_{t-2} - \mu_h) + \varepsilon_t^h, \quad \varepsilon_t^h \sim \mathcal{N}(0, w_h^2). \quad (4.21)$$

In this model, we assume that the characteristic roots associated with (ϕ_h, ρ_h) lie outside of the unit circle for the stationarity. Also, for the initial values, we assume that the unconditional distribution of h_1 and h_2 is: $h_1, h_2 \sim \mathcal{N}(\mu_h, (1 - \rho_h)w_h^2/(1 + \rho_h)((1 - \rho_h)^2 - \phi_h^2))$. It is obvious that, when $\rho_h = 0$, the model reduces to the standard SV model.

The SV-J model introduces rare but significant jumps in the mean equation just like the GARCH-J.

$$y_t = \mu + k_t q_t + \varepsilon_t^y, \quad \varepsilon_t^y \sim \mathcal{N}(0, \mathbf{e}_t^h), \quad (4.22)$$

$$h_t = \mu_h + \phi_h(h_{t-1} - \mu_h) + \varepsilon_t^h, \quad \varepsilon_t^h \sim \mathcal{N}(0, w_h^2). \quad (4.23)$$

Here, the jump variable $q_t \in \{0, 1\}$ is a Bernoulli variable with success probability $P(q_t = 1) = \kappa$, indicating the presence of a jump. Thus, $q_t = 1$ implies that a jump takes place at time t and its size is determined by k_t , which has the following distribution: $k_t \sim \mathcal{N}(\mu_k, \sigma_k^2)$.

Developed by (Koopman and Hol Uspensky, 2002), the SV-M model incorporates volatility into the mean equation to capture feedback effects:

$$y_t = \mu + \lambda e_t^h + \varepsilon_t^y, \quad \varepsilon_t^y \sim \mathcal{N}(0, e_t^h), \quad (4.24)$$

$$h_t = \mu_h + \phi_h(h_{t-1} - \mu_h) + \varepsilon_t^h, \quad \varepsilon_t^h \sim \mathcal{N}(0, w_h^2). \quad (4.25)$$

Here, λ captures the extent of volatility feedback. If $\lambda = 0$, the model reduces to the standard SV model.

In the SV-MA model, the observation equation is extended by adding MA(1)-type innovations:

$$y_t = \mu + \varepsilon_t^y, \quad (4.26)$$

$$\varepsilon_t^y = u_t + \psi u_{t-1}, \quad u_t \sim \mathcal{N}(0, e_t^h), \quad (4.27)$$

$$h_t = \mu_h + \phi_h(h_{t-1} - \mu_h) + \varepsilon_t^h, \quad \varepsilon_t^h \sim \mathcal{N}(0, w_h^2), \quad (4.28)$$

where $u_0 = 0$ and $|\psi| < 1$ ensures invertibility.

The SV-t model introduces heavy-tailed behavior through Student's t -distributed innovations:

$$y_t = \mu_t + \varepsilon_t^y, \quad \varepsilon_t^y \sim t_\nu(0, e_t^h), \quad (4.29)$$

$$h_t = \mu_h + \phi(h_{t-1} - \mu_h) + \varepsilon_t^h, \quad \varepsilon_t^h \sim \mathcal{N}(0, w_h^2). \quad (4.30)$$

where $u_0 = 0$ and $|\psi| < 1$ ensures invertibility. This model is useful for capturing large and infrequent shocks in return data.

The SV-L model accounts for the leverage effect, i.e., the asymmetry where negative returns increase future volatility more than positive ones. This is achieved by introducing a non-zero correlation between the return and volatility innovations:

$$y_t = \mu + \varepsilon_t^y, \quad \varepsilon_t^y \sim \mathcal{N}(0, e_t^h), \quad (4.31)$$

$$h_t = \mu_h + \phi_h(h_{t-1} - \mu_h) + \varepsilon_t^h, \quad \varepsilon_t^h \sim \mathcal{N}(0, w_h^2), \quad (4.32)$$

where ε_t^y and ε_t^h innovations follow a bivariate normal distribution:

$$\begin{pmatrix} \varepsilon_t^y \\ \varepsilon_t^h \end{pmatrix} \sim \mathcal{N}\left(\mathbf{0}, \begin{pmatrix} e_t^h & \rho e^{h_t/2} w_h \\ \rho e^{h_t/2} w_h & w_h^2 \end{pmatrix}\right) \quad (4.33)$$

When $\rho < 0$, negative shocks to returns lead to higher future volatility, consistent with the leverage effect observed in financial markets.

In summary, Table 4.2 provides an overview of the GARCH and Stochastic Volatility models utilized in this thesis.

Table 4.2: The List of GARCH and Stochastic Volatility Models.

GARCH MODELS	
GARCH	GARCH(1,1) model where σ_t^2 follows a stationary AR(1)
GARCH-2	same as GARCH but σ_t^2 follows a stationary AR(2)
GARCH-J	same as GARCH but the prices equation has a “jump” component
GARCH-M	same as GARCH but σ_t^2 enters the prices equation as a covariate
GARCH-MA	same as GARCH but but the observation error follows an MA(1)
GARCH-t	same as GARCH but but the observation error follows a t distribution
GARCH-GJR	GARCH with a leverage effect
STOCHASTIC VOLATILITY MODELS	
SV	stochastic volatility model where h_t follows a stationary AR(1)
SV-2	same as SV but h_t follows a stationary AR(2)
SV-J	same as SV but the prices equation has a “jump” component
SV-M	same as SV but h_t enters the prices equation as a covariate
SV-MA	same as SV but the observation error follows an MA(1)
SV-t	same as SV but the observation error follows a t distribution
SV-L	SV with a leverage effect

4.3 Bayesian Estimation Method

4.3.1 Gibbs Sampler

In this study, we adopt the methodological framework proposed by (Chan and Grant, 2016). The estimation of the GARCH and SV models is performed using the Markov Chain Monte Carlo (MCMC) approach. Specifically, Markov chain-based samplers are designed to approximate the posterior distributions of the model parameters. These posterior samples are subsequently employed to derive key quantities such as posterior means and marginal likelihoods.

For the SV models, the joint sampling of the log-volatility terms is conducted using the Metropolis-Hastings algorithm, following the precision sampler approach developed by (Chan and Jeliazkov, 2009) and (Chan, 2017). This method facilitates sampling from the conditional posterior distribution $p(h|y, \mu, \mu_h, \phi_h, \omega_h^2)$.

Similarly, for the GARCH models, Metropolis-Hastings algorithms are employed to sample from the conditional posterior distributions. For instance, in the standard GARCH model, the parameters are divided into two groups: μ and $\gamma = (\alpha_0, \alpha_1, \beta_1)$. Sampling proceeds by drawing sequentially from the conditional distributions $p(\mu|y, \gamma)$ and $p(\gamma|y, \mu)$. For sampling of μ , we use the Gaussian proposal distribution $N(\bar{y}, s^2/T)$, where \bar{y} is the sample mean and s^2/T is the sample variance. In order to sample γ , Gaussian proposal centered at the mode of $p(\gamma|y, \mu)$ with covariance matrix set to be the outer product of the scores is used. For the other GARCH models, additional parameters are sampled by extending the basic sampler with an extra block to accommodate the new parameter structure. See (Chan and Grant, 2016) for the further details on the Gibbs sampler.

4.3.2 Priors

In this thesis, we adopt prior specifications largely in line with (Chan and Grant, 2016). For both GARCH and SV models, the priors used for common parameters are mostly identical. All priors are proper but relatively noninformative.

For the standard GARCH, we assume independent priors for μ and $\gamma = (\alpha_0, \alpha_1, \beta_1)'$ specified as:

$$\mu \sim \mathcal{N}(\mu_0, V_\mu), \quad \log \gamma \sim \mathcal{N}(\gamma_0, V_\gamma) \mathbf{1}(\alpha_1 + \beta_1 < 1) \quad (4.34)$$

where, γ follows a truncated log-normal distribution that satisfies the stationarity condition $\alpha_1 + \beta_1 < 1$. The hyperparameters settings are defined as: $\mu_0 = 0$, $V_\mu = 10$, $\gamma_0 = (1, \log 0.1, \log 0.8)'$. These values set relatively uninformative priors with prior medians of $\mu = 0$ and $\gamma = (2.72, 0.1, 0.8)'$, consistent with empirical estimates in financial data.

For the GARCH-2, we employ the same prior for μ , but the prior for γ is modified: $\tilde{\gamma} = (\alpha_0, \alpha_1, \beta_1, \beta_2)'$ where $\log \tilde{\gamma} \sim \mathcal{N}(\tilde{\gamma}, V_{\tilde{\gamma}})\mathbf{1}(\alpha_1 + \beta_1 + \beta_2 < 1)$ with $\tilde{\gamma}_0 = (1, \log 0.1, \log 0.8, \log 0.1)'$ and $V_{\tilde{\gamma}} = \text{diag}(10, 1, 1, 1)$.

For the remaining GARCH models, the prior distributions for μ and γ are set as in equation (4.34), with specific additions for each model. In the GARCH-J specification, the jump intensity parameter κ is assigned a uniform prior over the range $(0, 0.1)$. Moreover, the pair $\delta = (\mu_k, \log \sigma_k^2)'$, representing the mean and variance of jump sizes, is assumed to follow a bivariate normal distribution, denoted as $\kappa \sim \mathcal{U}(0, 0.1)$ and $\delta \sim \mathcal{N}(\delta_0, V_{\delta})$. To center the average jump size at zero, we set $\delta_0 = (0, \log 10)'$ and $V_{\delta} = \text{diag}(10, 1)$.

In the GARCH-M framework, the volatility feedback coefficient λ is given a normal prior: $\lambda \sim \mathcal{N}(\lambda_0, V_{\lambda})$, where $\lambda_0 = 0$ and $V_{\lambda} = 100$. For the GARCH-MA model, the MA(1) parameter ψ follows a truncated normal distribution confined within $(-1, 1)$: $\psi \sim \mathcal{N}(\psi_0, V_{\psi})\mathbf{1}(|\psi| < 1)$, with $\psi_0 = 0$ and $V_{\psi} = 1$.

Turning to the GARCH-t model, the degrees of freedom parameter ν is assumed to follow a uniform distribution on the interval $(2, 100)$, i.e., $\nu \sim \mathcal{U}(2, 100)$, ensuring the existence of the first two moments of the t -distribution. Finally, in the GARCH-GJR specification, the leverage parameter δ_1 is assigned a uniform prior conditional on γ , maintaining positivity and stationarity in the variance process. Specifically, the constraints $\alpha_1 + \delta_1 > 0$ and $\alpha_1 + \beta_1 + \delta_1 < 1$ are applied, resulting in the conditional prior $(\delta_1 | \gamma) \sim \mathcal{U}(-\alpha_1, 1 - \alpha_1 - \beta_1)$.

Moving on to the stochastic volatility (SV) models, we apply a consistent set of hyperparameters for shared parameters across models. In the basic SV specification, we assign independent priors to μ , μ_0 , ϕ_h , and w_h^2 .

$$\begin{aligned} \mu &\sim \mathcal{N}(\mu_0, V_{\mu}), & \mu_h &\sim \mathcal{N}(\mu_{h0}, V_{\mu_h}) \\ \phi_h &\sim \mathcal{N}(\phi_{h0}, V_{\phi_h}), & w_h^2 &\sim IG(\nu_h, S_h) \end{aligned} \tag{4.35}$$

Here, $IG(\cdot)$ refers to the inverse-gamma distribution. To align the volatility behavior with that observed in GARCH models, the hyperparameters are set as follows: $\mu_0 = 0$, $\mu_{h0} = 1$, $V_\mu = V_{\mu_h} = 10$, $\phi_{h0} = 0.97$, $V_{\phi_{h0}} = 0.1^2$, $v_h = 5$, and $S_h = 0.16$.

In the case of the SV-2 model, we retain the same priors for μ , μ_0 , and w_h^2 as specified in equation (6.2), but replace the prior for ϕ_h with $\theta_h = (\phi_h, \rho_h)'$. Here, we assume $\theta_h \sim \mathcal{N}(\theta_{h0}, V_{\theta_h})\mathbf{1}(\theta_h \in A)$, where $\theta_{h0} = (0.97, 0)'$, $V_{\theta_h} = \text{diag}(0.1^2, 1)$, and $A \subset \mathbb{R}^2$ defines the set where the characteristic polynomial's roots, defined by θ_h , lie outside the unit circle.

For the other SV models, the prior distributions assigned to μ , μ_0 , ϕ_h , and w_h^2 remain consistent with those in equation (6.2), while any additional parameters adopt the same prior structures as their GARCH counterparts. Lastly, for the SV-L model, the correlation parameter ρ is given a uniform prior: $\rho \sim \mathcal{U}(-1, 1)$.

4.3.3 Comparison of Models

To compare the volatility models in this thesis, we use Bayes factors, following the approach of (Chan and Grant, 2016) and (Tiwari et al., 2019). Bayes factors are computed using importance sampling, which is particularly useful because it is easy to implement, allows straightforward computation of numerical standard errors, and only requires evaluation of the prior and the likelihood function.

For a set of models $(M_1, M_2, M_3, \dots, M_K)$, each model is divided into two distinct parts: likelihood function and prior density. The likelihood function $p(y|\theta_k, M_k)$ depends on the model-specific parameter vector θ_k of dimension p_k where prior density is $p(\theta_k|M_k)$.

The Bayes factor in favor of model M_i against M_j is defined as:

$$BF = \frac{p(y|M_i)}{p(y|M_j)}, \quad (4.36)$$

where the marginal likelihood is:

$$p(y|M_k) = \int p(y|\theta_k, M_k) p(\theta_k|M_k) d\theta_k, \quad (4.37)$$

where $p(y|\theta_k, M_k)$ is the likelihood function of the observed data y . The marginal likelihood function $p(y|M_k)$ reflects how well model M_k explains observed data y . A higher value indicates better model fit. If $BF > 1$, it suggests that the observed data are more likely from model M_i comparing to M_j . This shows that model M_i is in favor of model M_j . For instance, if a Bayes factor is 4, this implies that M_i is 4 times more likely than model M_j given the data.

Bayes factors also relate to posterior odds via:

$$\frac{P(M_i|y)}{P(M_j|y)} = \frac{P(M_i)}{P(M_j)} \times BF_{i,j}, \quad (4.38)$$

where, $\frac{P(M_i)}{P(M_j)}$ denotes the prior odds ratio. If both models are equally likely a priori, then posterior odd ratio would equal the Bayes factor.

Since the Bayes factor is simply the ratio of two marginal likelihoods, it is sufficient to compute the marginal likelihoods for the set of competing models. However, the marginal likelihood functions generally do not have closed-form solutions for all models. To overcome this, the marginal likelihoods of the GARCH and SV models are estimated using the improved cross-entropy method proposed by (Chan and Eisenstat, 2015) and applied by (Chan and Grant, 2016), as the integral in Equation (5) is typically high-dimensional and computationally intractable.

4.4 Comparison of Volatility Models

Table 4.3: Log Marginal Likelihoods of the GARCH and SV Models of Bitcoin and Ethereum.

	Bitcoin	Ethereum
GARCH	-7155.4(0.02)	-7381.9(0.01)
SV	-6892.5(0.40)	-7316.9(0.07)
GARCH-2	-7156.6(0.09)	Convergence Problem
SV-2	-6994.2(0.36)	-7313.2(0.12)
GARCH-J	-6885.8(0.13)	-7322.6(0.10)
SV-J	-6889.4(0.52)	-7322.9(0.52)
GARCH-M	-7163.0(0.07)	-7389.2(0.07)
SV-M	-6901.0 (0.23)	-7323.5(0.14)
GARCH-MA	-7158.7(0.13)	-7383.9(0.05)
SV-MA	-6893.1(0.29)	-7315.4(0.01)
GARCH-t	-6835.8 (0.01)	-7306.0(0.04)
SV-t	-6825.8(0.21)	-7294.8(0.02)
GARCH-GJR	-7148.6(0.03)	-7385.8(0.05)
SV-L	-6897.1(0.36)	Convergence Problem

All models are estimated using the Bayesian estimation method described in Section 6.1. The marginal likelihoods of the GARCH and SV models are computed using the improved cross-entropy method developed by (Chan and Eisenstat, 2015) and applied by (Chan and Grant, 2016).

Table 4.3 presents the log marginal likelihood values of the SV and GARCH models for Bitcoin and Ethereum.

For Bitcoin, as shown in Table 4.3, all SV models-except for SV-J-outperform their GARCH counterparts. In SV models, log-volatility is treated as a latent random variable, whereas in GARCH models, the conditional variance is a deterministic function of past data and parameters. This stochastic treatment of volatility makes SV models more robust to model misspecification and structural shifts in the data, explaining their superior performance.

Among the 14 models for Bitcoin, the SV-t model performs best, with the highest log marginal likelihood value of -6825.8. The GARCH-t model ranks second overall and has the highest value among all GARCH models. This result highlights the advantage

of the heavy-tailed t -distribution in capturing extreme return behavior. Additionally, the standard GARCH model slightly outperforms GARCH-2, and the SV model outperforms SV-2, suggesting that an AR(1) specification is sufficient for modeling Bitcoin volatility. Jump component for both type of models improve the fitness of the model which is consistent with the (Chan and Grant, 2016) results. Volatility feedback is not important for the estimation of GARCH and SV models. Moreover, the standard GARCH and SV models outperform GARCH-MA and SV-MA, respectively. This suggests that moving average innovations do not provide a significant marginal benefit. The GARCH-GJR model, which incorporates a leverage effect, performs better than the standard GARCH model. However, its SV counterpart, SV-L, does not improve upon the performance of the standard SV model.

For Ethereum, the GARCH-2 and SV-L models are excluded due to convergence problems. Similar to the Bitcoin results, the SV-t model achieves the highest log marginal likelihood (-7294.8), confirming its superiority in capturing Ethereum's volatility. However, unlike in the Bitcoin case, the SV-2 model performs better than the standard SV model, indicating that an AR(2) structure provides additional explanatory power for Ethereum. Among the GARCH-family models, the GARCH-t model again performs best and is the second-best model overall. Also, jump component improves the GARCH model, whereas it doesn't increase the performance of standard SV model like (Tiwari et al., 2019) findings. Similar to Bitcoin, the volatility feedback effect does not improve the estimation performance of either model class. While the moving average parameter enhances the performance of the standard SV model, it has no significant effect on the GARCH model. The leverage effect is unimportant for both GARCH and SV models, which is also in line with the results of (Tiwari et al., 2019). This implies that Ethereum does not behave in the same way as traditional stock markets. In summary, the marginal likelihood estimates show that SV models generally outperform their GARCH counterparts, with the exception of the SV-J model.

4.5 Estimation Results

This section presents the posterior estimates of model parameters for both Bitcoin and Ethereum.

Table 4.4 reports the posterior mean estimates of the GARCH model parameters for Bitcoin. The β_1 estimates vary between 0.79 and 0.93, indicating substantial persistence. Notably, the GARCH-2 model yields the lowest β_1 estimate at 0.79; however, when combining $\beta_1 + \beta_2$ (0.86), its persistence aligns with that of the other GARCH models. The average jump size μ_k is estimated at -0.17, while the jump intensity κ is 0.10, suggesting roughly 36 jumps per year in the Bitcoin daily dataset. The estimated GARCH-M parameter λ is 0.01, indicating positive volatility feedback, though it lacks statistical significance. Furthermore, the δ_1 estimate surpasses λ and ψ , which is consistent with the superior marginal likelihood observed for the GARCH-GJR model. The GARCH-t model's estimated degrees of freedom ν is 2.89, reflecting heavy-tailed behavior and indicating greater robustness relative to other GARCH specifications based on marginal likelihood rankings. In the GARCH-MA model, the ψ estimate is 0.01 but lacks statistical significance, suggesting no meaningful improvement over the standard GARCH model. The positive δ_1 estimate in the GARCH-GJR model reinforces its advantage over the basic GARCH framework.

Table 4.5 presents the posterior parameter estimates for the SV models applied to Bitcoin. Similar to the GARCH models, the ϕ_h values range between 0.89 and 0.98, signaling strong persistence. In the SV-MA model, the ψ coefficient is significantly negative, excluding zero at the 95% confidence level, indicating that the SV-MA model underperforms relative to the basic SV model. Unlike the GARCH models, however, the SV-J model produces a positive estimate for the jump size parameter μ_k (2.75). The SV-M model's feedback coefficient λ is estimated near zero, suggesting feedback effects play no meaningful role in Bitcoin's volatility dynamics. Additionally, the degrees of freedom parameter ν in the SV-t model is 7.87, indicating thinner tails compared to the GARCH-t specification and resembling a distribution closer to normality.

Table 4.6 shows the posterior parameter estimates for the GARCH models applied to Ethereum. Similar to Bitcoin, β_1 estimates fall between 0.93 and 0.95, reflecting high persistence. The estimated jump intensity κ is 0.09, implying around 32 jumps annually. However, differing from Bitcoin, the average jump size μ_k is positive (0.49),

and λ is estimated at zero, indicating that feedback effects are not significant in modeling Ethereum volatility. Moreover, δ_1 is close to zero, suggesting the leverage effect is negligible, thereby supporting the superiority of the standard GARCH model over the GARCH-GJR variant for Ethereum. For the GARCH-t model, the estimated degrees of freedom ν is 4.65, which reflects heavy tails but is less extreme than the Bitcoin estimate. The MA(1) coefficient ψ is -0.03 and does not exclude zero at the 95% confidence level, indicating that the GARCH-MA model offers no significant improvement over the standard GARCH framework.

Table 4.7 presents the posterior mean estimates for Ethereum's SV models. As observed with Bitcoin, the ϕ_h parameter points to high persistence. The volatility feedback coefficient λ is estimated at 0.01, suggesting potential relevance of feedback in Ethereum volatility; however, it is not statistically significant at the 5% level. The jump intensity estimate κ of 0.09 aligns with the GARCH-J result, while the estimated jump size μ_k is positive (0.91). The SV-t model yields a degrees of freedom estimate ν of 6.65, higher than the GARCH-t estimate, indicating thinner tails and closer resemblance to a normal distribution. The ψ coefficient in the SV-MA model is -0.06, and its 95% interval excludes zero, suggesting that SV-MA outperforms the standard SV model for Ethereum.

Lastly, two diagnostic checks were conducted: the Ljung-Box and McLeod-Li statistics of order 20, denoted as $Q(20)$ and $Q^2(20)$, respectively, were computed using the standardized residuals and squared residuals. The 5% and 1% critical values are 31.41 and 37.57. For both Bitcoin and Ethereum, none of the Ljung-Box tests reject the null hypothesis of no serial correlation at the 1% level, indicating the models effectively remove autocorrelation in the residuals.

For Bitcoin, all GARCH models pass the McLeod-Li test at the 5% significance level, confirming their ability to capture time-varying volatility. Among SV models, all except the basic SV pass the McLeod-Li test at the 1% level, supporting their adequacy in modeling volatility. Regarding Ethereum, the McLeod-Li tests fail to reject the null hypothesis at the 5% level across all models, demonstrating that both GARCH and SV models satisfactorily capture Ethereum's time-varying volatility.

Table 4.4: Posterior means and Posterior standard deviations (in parentheses) for GARCH models: Bitcoin.

	GARCH	GARCH-2	GARCH-J	GARCH-M	GARCH-MA	GARCH-t	GARCH-GJR
μ	0.15 (0.06)	0.15 (0.06)	0.09 (0.05)	0.05 (0.10)	0.15 (0.06)	0.08 (0.04)	0.10 (0.06)
α_0	0.63 (0.06)	0.66 (0.08)	0.02 (0.00)	0.60 (0.09)	0.64 (0.11)	0.03 (0.02)	0.70 (0.10)
α_1	0.10 (0.01)	0.11 (0.01)	0.02 (0.00)	0.09 (0.01)	0.10 (0.01)	0.03 (0.00)	0.07 (0.01)
β_1	0.86 (0.01)	0.79 (0.02)	0.93 (0.00)	0.87 (0.02)	0.86 (0.02)	0.93 (0.01)	0.85 (0.02)
β_2		0.07 (0.01)					
κ			0.10 (0.00)				
μ_k			-0.17 (0.39)				
σ_k^2			54.38 (8.35)				
λ				0.01 (0.01)			
ψ					0.01 (0.02)		
ν						2.89 (0.21)	
δ_1							0.08 (0.01)
$Q(20)$	16.75	16.52	23.52	16.62	16.61	20.8	17.76
$Q^2(20)$	7.09	7.32	8.24	7.32	7.39	8.72	8.04

Figure 4.15 to Figure 4.40 illustrate the return volatility graphs of each GARCH and SV model for Bitcoin and Ethereum. As discussed earlier, the SV-t model provides the best fit for both Bitcoin and Ethereum price returns. Therefore, we focus on the volatility graph of the price returns of these two cryptocurrencies.

Figure 4.38 displays the return volatility graph of the SV-t model for Bitcoin. The graph shows notable spikes in volatility during the periods 2018–2019 and in 2020.

Table 4.5: Posterior means and Posterior standard deviations (in parentheses) for SV models: Bitcoin.

	SV	SV-2	SV-J	SV-M	SV-MA	SV-t	SV-L
μ	0.06 (0.05)	0.08 (0.04)	0.04 (0.05)	0.05 (0.06)	0.09 (0.06)	0.08 (0.05)	0.05 (0.04)
μ_h	1.99 (0.10)	2.11 (0.25)	1.91 (0.23)	2.03 (0.11)	2.00 (0.10)	1.97 (0.28)	2.08 (0.10)
ϕ_h	0.89 (0.02)	0.90 (0.15)	0.97 (0.01)	0.91 (0.02)	0.90 (0.01)	0.98 (0.01)	0.90 (0.01)
ω_h^2	0.25 (0.04)	0.16 (0.06)	0.06 (0.01)	0.21 (0.04)	0.24 (0.01)	0.04 (0.01)	0.22 (0.01)
ρ_h		0.05 (0.13)					
κ			0.07 (0.02)				
μ_k			2.75 (0.65)				
σ_k^2			38.28 (11.22)				
λ				0.00 (0.01)			
ψ					-0.06 (0.02)		
ν						7.87 (2.75)	
ρ							-0.15 (0.02)
$Q(20)$	19.90	15.65	18.70	20.81	20.44	23.98	18.38
$Q^2(20)$	49.95	35.14	27.54	25.10	36.17	18.34	30.06

These spikes correspond to the 2018 Bitcoin crash and the global financial uncertainty caused by the COVID-19 pandemic in 2020. Between 2021 and 2023, Bitcoin's volatility declined, indicating a relatively stable market. However, between 2023 and 2024, volatility increased again, followed by a decline after 2024.

Table 4.6: Posterior means and Posterior standard deviations (in parentheses) for GARCH models: Ethereum.

	GARCH	GARCH-2	GARCH-J	GARCH-M	GARCH-MA	GARCH-t	GARCH-GJR
μ	0.14 (0.07)	- (-)	0.09 (0.07)	0.07 (0.16)	0.14 (0.07)	0.10 (0.06)	0.14 (0.07)
α_0	0.16 (0.05)	- (-)	0.02 (0.01)	0.16 (0.01)	0.14 (0.05)	0.04 (0.03)	0.17 (0.04)
α_1	0.04 (0.01)	- (-)	0.05 (0.01)	0.04 (0.01)	0.04 (0.01)	0.04 (0.01)	0.04 (0.01)
β_1	0.95 (0.01)	- (-)	0.93 (0.01)	0.95 (0.01)	0.95 (0.01)	0.94 (0.01)	0.95 (0.01)
β_2		- (-)					
κ			0.09 (0.01)				
μ_k			0.49 (0.57)				
σ_k^2			39.90 (8.82)				
λ				0.00 (0.01)			
ψ					-0.03 (0.02)		
ν						4.65 (0.44)	
δ_1							-0.00 (0.01)
$Q(20)$	27.08	-	25.95	27.23	27.06	26.33	27.31
$Q^2(20)$	17.05	-	19.86	17.57	17.85	18.41	18.64

Figure 4.40 presents the return volatility graph of the SV-t model for Ethereum. The graph shows a decreasing trend in volatility until 2018, after which volatility spikes occurred—similar to Bitcoin—in 2018 and 2020. Between 2021 and 2022, Ethereum’s return volatility decreased, but it rose again in 2022. Like Bitcoin, Ethereum experienced a relatively calm market from 2022 to 2023. After 2023, however, Ethereum’s volatility exhibits an upward trend.

Table 4.7: Posterior means and Posterior standard deviations (in parentheses) for SV models: Ethereum.

	SV	SV-2	SV-J	SV-M	SV-MA	SV-t	SV-L
μ	0.11 (0.06)	0.10 (0.06)	0.03 (0.06)	0.04 (0.10)	0.11 (0.06)	0.08 (0.05)	- (-)
μ_h	2.55 (0.10)	2.52 (0.11)	2.36 (0.17)	2.55 (0.10)	2.53 (0.10)	2.29 (0.28)	- (-)
ϕ_h	0.95 (0.01)	0.99 (0.11)	0.98 (0.01)	0.94 (0.01)	0.95 (0.01)	0.98 (0.01)	- (-)
ω_h^2	0.07 (0.01)	0.10 (0.03)	0.04 (0.02)	0.07 (0.01)	0.07 (0.02)	0.03 (0.01)	- (-)
ρ_h		-0.07 (0.13)					
κ			0.09 (0.01)				
μ_k			0.91 (0.57)				
σ_k^2			24.94 (4.59)				
λ				0.01 (0.01)			
ψ					-0.06 (0.02)		
ν						6.65 (1.09)	
ρ							
$Q(20)$	21.76	30.53	23.67	26.77	20.79	29.29	-
$Q^2(20)$	21.71	30.79	20.48	23.65	20.75	16.46	-

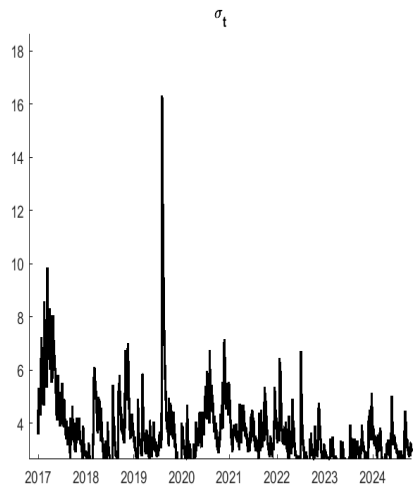


Figure 4.15: Return Volatility Graph of Bitcoin: Standard GARCH Model.

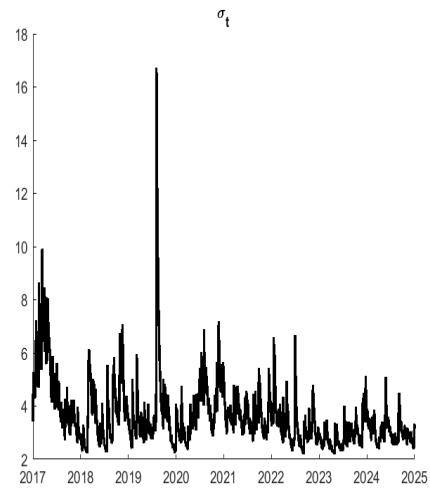


Figure 4.16: Return Volatility Graph of Bitcoin: GARCH-2 Model.

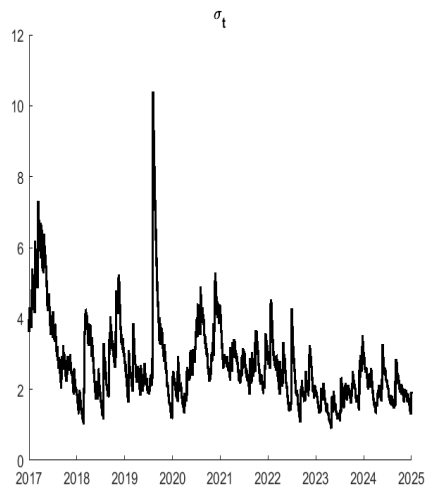


Figure 4.17: Return Volatility Graph of Bitcoin: GARCH-J Model.

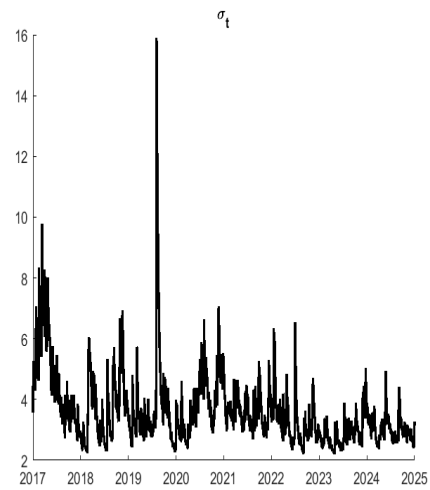


Figure 4.18: Return Volatility Graph of Bitcoin: GARCH-M Model.

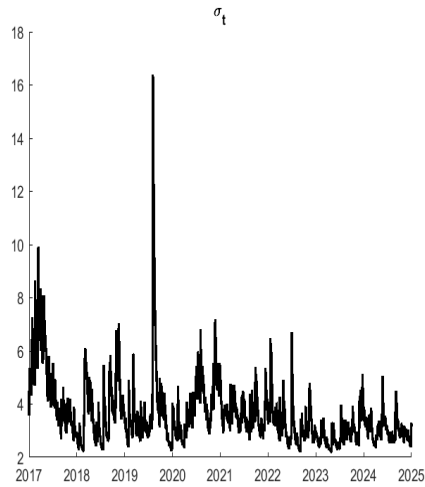


Figure 4.19: Return Volatility Graph of Bitcoin: GARCH-MA Model.

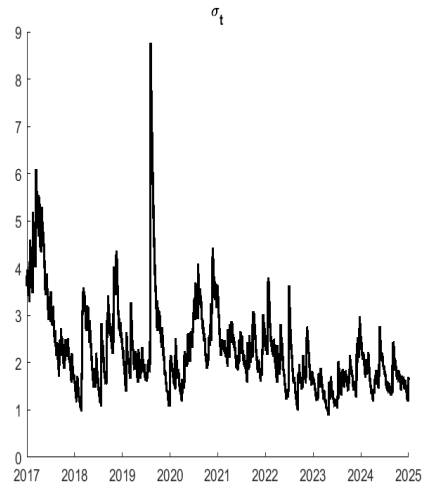


Figure 4.20: Return Volatility Graph of Bitcoin: GARCH-GJR Model.

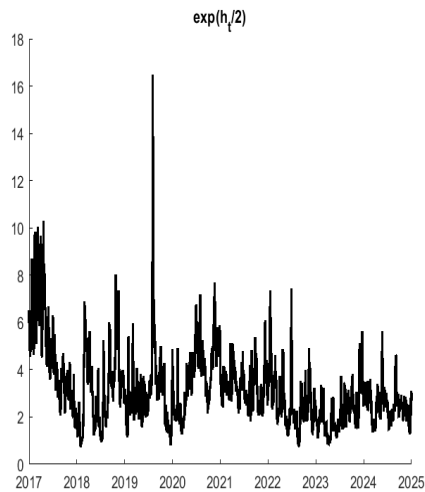


Figure 4.21: Return Volatility Graph of Bitcoin: Standard SV Model.

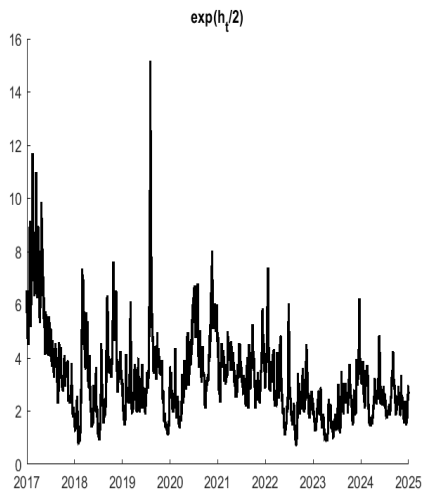


Figure 4.22: Return Volatility Graph of Bitcoin: SV-2 Model.

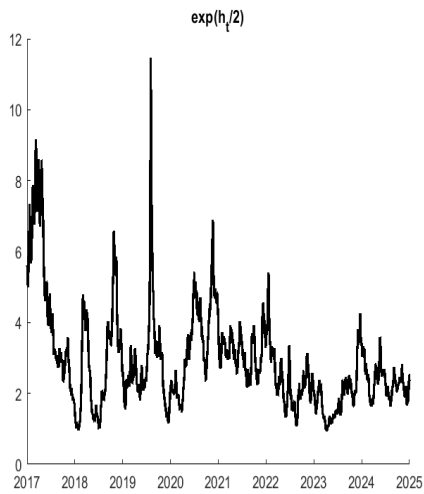


Figure 4.23: Return Volatility Graph of Bitcoin: SV-J Model.

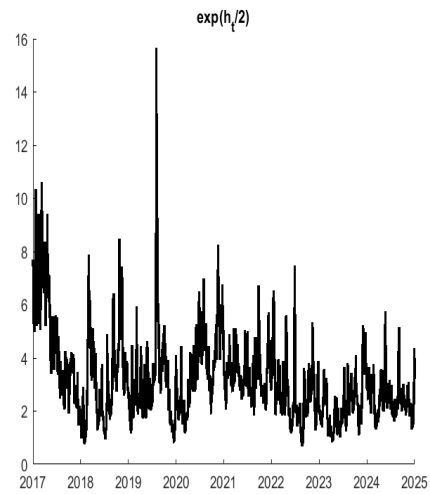


Figure 4.24: Return Volatility Graph of Bitcoin: SV-M Model.

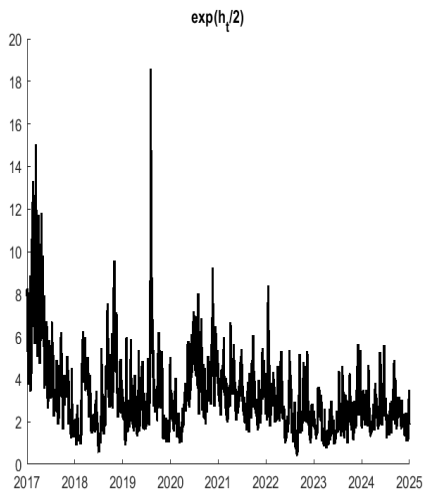


Figure 4.25: Return Volatility Graph of Bitcoin: SV-MA Model.

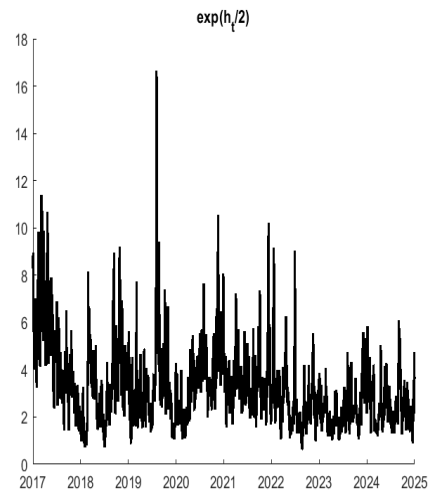


Figure 4.26: Return Volatility Graph of Bitcoin: SV-L Model.

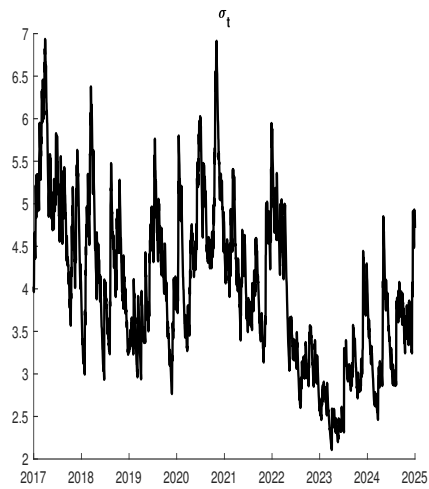


Figure 4.27: Return Volatility Graph of Ethereum: Standard GARCH Model.

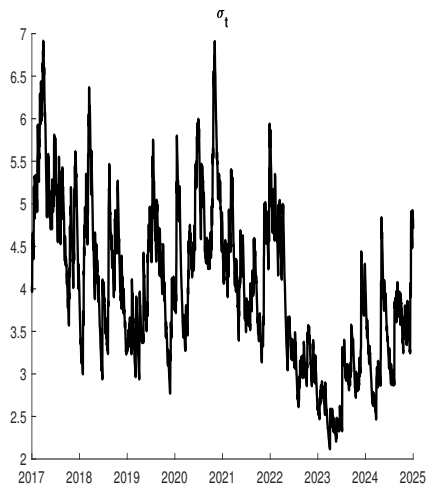


Figure 4.28: Return Volatility Graph of Ethereum: GARCH-M Model.

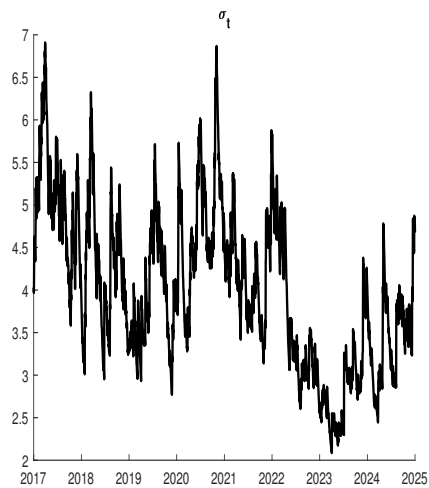


Figure 4.29: Return Volatility Graph of Ethereum: GARCH-MA Model.

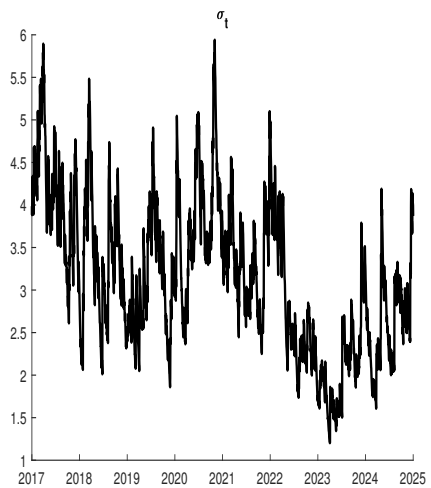


Figure 4.30: Return Volatility Graph of Ethereum: GARCH-t Model.

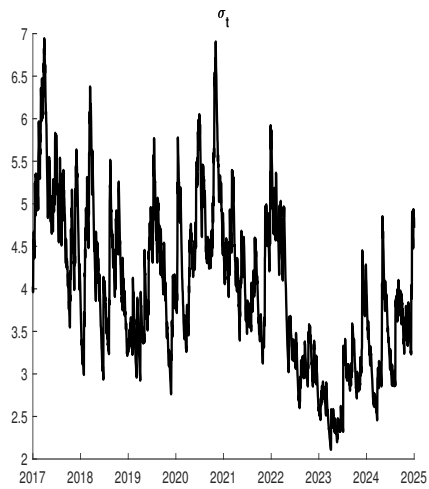


Figure 4.31: Return Volatility Graph of Ethereum: GARCH-GJR Model.

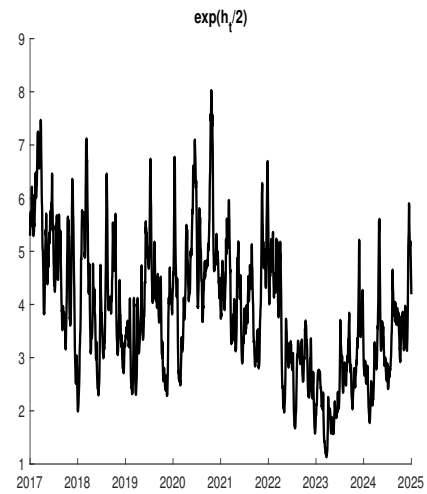


Figure 4.32: Return Volatility Graph of Ethereum: Standard SV Model.

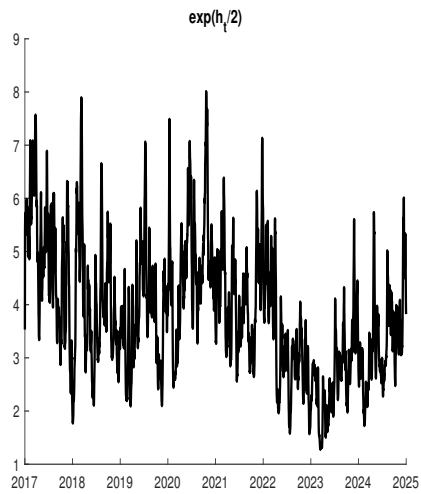


Figure 4.33: Return Volatility Graph of Ethereum: SV-2 Model.

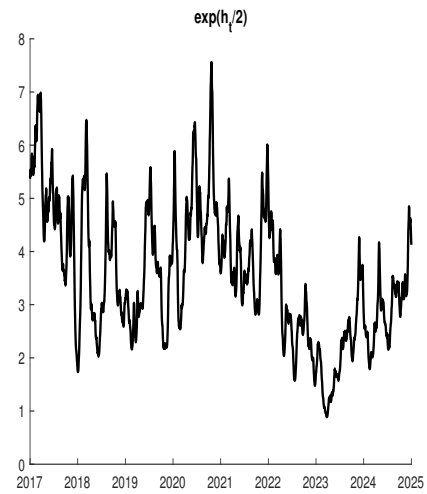


Figure 4.34: Return Volatility Graph of Ethereum: SV-J Model.

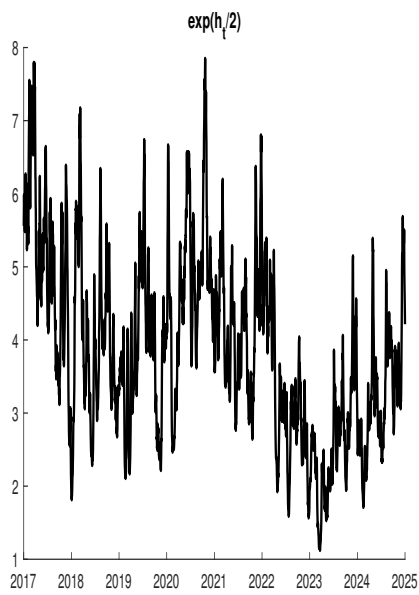


Figure 4.35: Return Volatility Graph of Ethereum: SV-M Model.

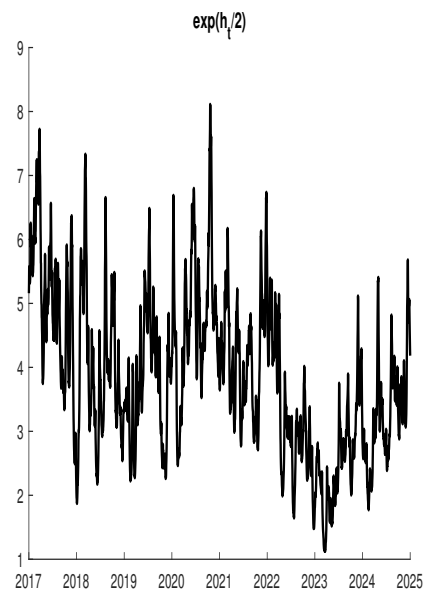


Figure 4.36: Return Volatility Graph of Ethereum: SV-MA Model.

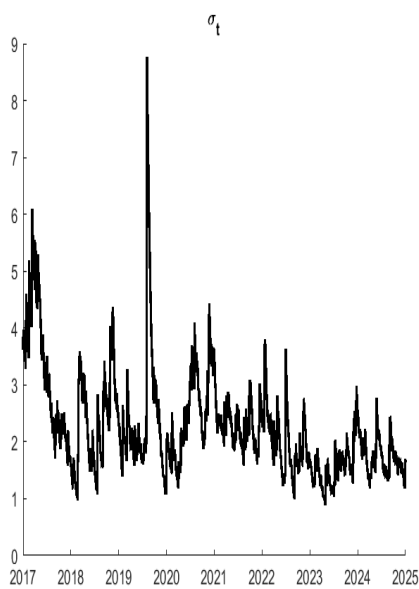


Figure 4.37: Return Volatility Graph of Bitcoin: GARCH-t Model.

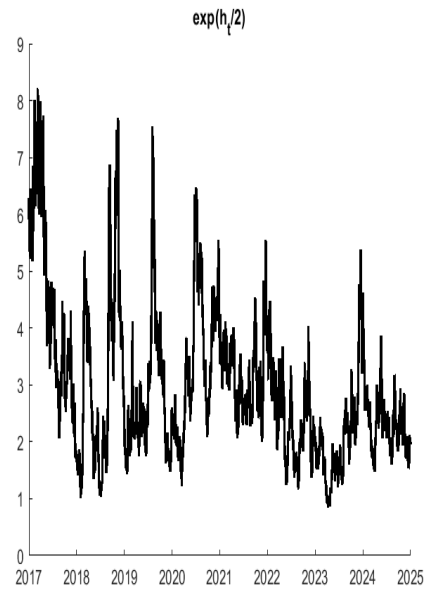


Figure 4.38: Return Volatility Graph of Bitcoin: SV-t Model.

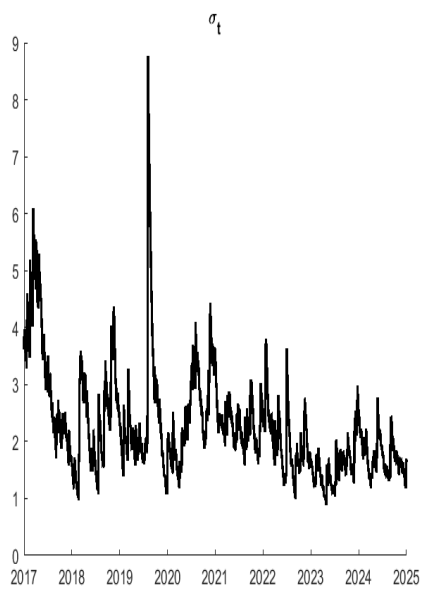


Figure 4.39: Return Volatility Graph of Ethereum: GARCH-J Model.

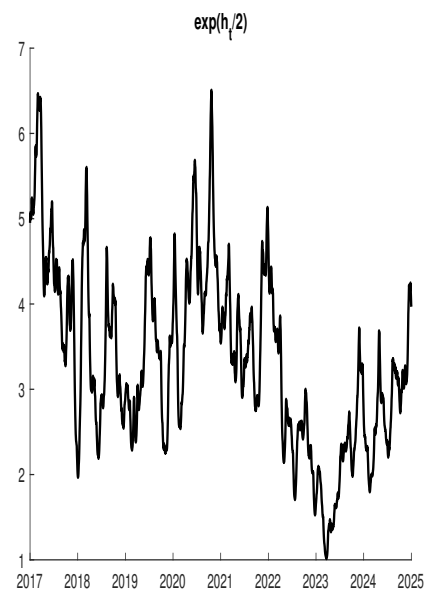


Figure 4.40: Return Volatility Graph of Ethereum: SV-t Model.

5. FORECASTING RESULTS

For the forecasting analyses, we conduct a recursive out-of-sample forecasting exercise to evaluate the performance of the GARCH and SV models. These models are compared based on their volatility forecasts and their ability to estimate Values-At-Risk (VaR), which is defined as the tail quantiles of the return densities. In this thesis, we compare the GARCH and SV models by using the entire forecast densities and computing the log predictive score (Fan et al., 2008), (Hung et al., 2008).

Given the data up to time t , denoted by $y_{1:t}$, the one-step-ahead predictive density $p(y_{t+1}|y_{1:t})$ under a given model is computed. We treat this predictive density as the forecast distribution for y_{t+1} . The forecast is evaluated by the log predictive likelihood $\log p(y_{t+1} | y_{1:t})$, which is the log of the predictive density evaluated at the observed value y_{t+1}^o . If the realized value y_{t+1}^o is likely under the forecast distribution, then the log predictive likelihood will be high; otherwise, it will be low.

This process is repeated recursively: after forecasting y_{t+1} , the dataset is expanded to $y_{1:t+1}$, and the next forecast is made. The log predictive score over the evaluation period $t_0 + 1, \dots, T$ is explained as the sum of the log predictive likelihoods:

$$\sum_{t=t_0}^{T-1} \log p(y_{t+1} = y_{t+1}^o | y_{1:t}) \quad (5.1)$$

A higher log predictive score indicates better forecast performance (Geweke and Amisano, 2011). The forecasting results for the GARCH and SV models are presented in Table 5.1:

Table 5.1 shows that the GARCH-t model provides the best volatility forecast for Bitcoin, as it records the highest log predictive score of -414.8 among all GARCH and SV models. Since GARCH-t also ranks second in terms of log marginal likelihood, its strong performance in volatility forecasting is expected. Among the

Table 5.1: Log Predictive Results of the GARCH and SV Models of Bitcoin and Ethereum

	Bitcoin	Ethereum
GARCH	-422.4	-411.5
SV	-423.2	-408.6
GARCH-2	-422.5	Convergence Problem
SV-2	-418.6	-409.8
GARCH-J	-419.1	-406.5
SV-J	-419.9	-408.5
GARCH-M	-422.3	-411.6
SV-M	-419.0	-410.3
GARCH-MA	-422.3	-411.4
SV-MA	-420.7	-408.4
GARCH-t	-414.8	-407.0
SV-t	-419.7	-407.7
GARCH-GJR	-422.3	-411.8
SV-L	-420.7	Convergence Problem

SV models, SV-2 delivers the best forecasting performance, surpassing both its SV counterparts and its GARCH analogue, GARCH-2. Although the SV-t model is the best performer in terms of log marginal likelihood, it is outperformed in forecasting by GARCH-t, SV-2, SV-M, and GARCH-J. t -distributed innovations significantly improve the GARCH and SV forecasts. When comparing each SV model with its corresponding GARCH counterpart, four SV models: SV-2, SV-M, SV-MA, and SV-L-achieve higher log predictive scores than their respective GARCH counterparts (GARCH-2, GARCH-M, GARCH-MA, and GARCH-GJR), and vice versa in the remaining cases. Incorporating a jump component substantially improves forecasting accuracy for both model families. Moreover, the volatility feedback channel and moving average innovations in SV models lead to improved forecasts compared to the standard SV model, while offering slight improvements in GARCH models. The leverage effect is particularly beneficial for SV models and provides minor gains in the GARCH framework.

In contrast, the volatility forecasting results for Ethereum differ significantly. The GARCH-J model provides the best performance, suggesting that incorporating a jump

component substantially improves forecasting accuracy. Despite its relatively poor log marginal likelihood compared to several other models, GARCH-J achieves the highest log predictive score of -406.5. The second-best model is another GARCH-type model, GARCH-t, which is consistent with its strong log marginal likelihood. Similar to the jump component, using t -distributed innovations enhances forecasting performance within the GARCH framework. However, the volatility feedback effect appears to have no significant impact on Ethereum returns for either model class. Additionally, the moving average component offers slight improvements in forecast accuracy for both GARCH and SV models. The leverage effect does not play a substantial role in forecasting Ethereum volatility. Unlike in the Bitcoin case, SV-t performs best among the SV models for Ethereum. However, SV-2 performs worse than SV, indicating that the AR(2) specification does not provide additional forecasting benefits for Ethereum returns.



6. CONCLUSION

In this thesis, we investigate the volatility of Bitcoin and Ethereum using GARCH and SV models. We consider seven GARCH and seven SV models and compare their estimation and forecasting performances for each cryptocurrency. To evaluate the models' estimation and forecasting capabilities, we apply Bayesian estimation techniques using daily data.

In the estimation phase, we compute the log marginal likelihoods for each GARCH and SV model and estimate the posterior means of their parameters. The results show that the SV- t model provides the best fit for both Bitcoin and Ethereum, suggesting that SV models are more robust to model misspecification and abrupt changes. The GARCH- t model ranks second for both cryptocurrencies, indicating that incorporating the heavy tails of the t -distribution considerably improves the performance of both GARCH and SV frameworks. Furthermore, the AR(2) process performs worse than AR(1) for Bitcoin, whereas the opposite holds for Ethereum. The inclusion of jump components generally improves the fit for both standard GARCH and SV models, except in the case of the standard SV model for Ethereum. The volatility feedback channel is found to be insignificant in all models. Moving average innovations enhance performance only for the standard SV model applied to Ethereum. Lastly, the leverage effect improves model performance in GARCH specifications for Bitcoin but remains insignificant for Ethereum, implying that Ethereum exhibits return dynamics distinct from those of traditional equity markets. We also calculate the posterior means of the model parameters.

In the forecasting phase, we evaluate each model by computing the log predictive scores based on the full predictive densities. Among the evaluated models, GARCH- t shows the strongest forecasting capability for Bitcoin, whereas GARCH-J emerges as the top performer for Ethereum. The AR(2) process significantly improves the standard SV models for Bitcoin price returns, whereas in the case of Ethereum, it

is found to make no substantial contribution to forecasting accuracy. Incorporating a jump component improves forecasts across both GARCH and SV models and offers marginal gains for Ethereum within the SV framework. The volatility feedback channel is relevant for Bitcoin forecasts in SV models and slightly improves the standard GARCH model, but it has no notable effect on Ethereum. Moving average innovations provide slight improvements in GARCH models for both assets and are beneficial in SV models for Ethereum, with a more pronounced effect in Bitcoin forecasting. The inclusion of t -distributed innovations enhances the forecasting ability of both standard GARCH and SV models. Finally, the leverage effect remains unimportant for Ethereum forecasts but contributes positively to forecast accuracy for Bitcoin in both model classes.

For future research, we recommend comparing GARCH and SV models with alternative approaches such as HAR (Heterogeneous Autoregressive) models, Score-Driven models, and Markov Switching GARCH models, incorporating various innovation distributions including the skewed normal (snorm) and generalized error distribution (ged). It would be interesting to see the comparisons of model performance within the Bayesian estimation framework, particularly in terms of both estimation accuracy and forecasting ability.

REFERENCES

- 1 **Nakamoto, S.** (2008). Bitcoin: A peer-to-peer electronic cash system.
- 2 **Nica, O., Piotrowska, K. and Schenk-Hoppé, K.R.,** (2022). Cryptocurrencies: Concept and current market structure, *Cryptofinance: A new currency for a new economy*, World Scientific, pp.1–28.
- 3 **Endri, E., Aipama, W., Razak, A., Sari, L. and Septiano, R.** (2021). Stock price volatility during the COVID-19 pandemic: The GARCH model, *Investment Management & Financial Innovations*, 18(4), 12.
- 4 **Aliyev, F., Ajayi, R. and Gasim, N.** (2020). Modelling asymmetric market volatility with univariate GARCH models: Evidence from Nasdaq-100, *The Journal of Economic Asymmetries*, 22, e00167.
- 5 **Qu, Z. and Perron, P.** (2013). A stochastic volatility model with random level shifts and its applications to S&P 500 and NASDAQ return indices, *The Econometrics Journal*, 16(3), 309–339.
- 6 **Chan, J.C. and Grant, A.L.** (2016). Modeling energy price dynamics: GARCH versus Stochastic Volatility, *Energy Economics*, 54, 182–189.
- 7 **Tiwari, A.K., Kumar, S. and Pathak, R.** (2019). Modelling the dynamics of Bitcoin and Litecoin: GARCH versus stochastic volatility models, *Applied Economics*, 51(37), 4073–4082.
- 8 **Yu, J.** (2002). Forecasting volatility in the New Zealand stock market, *Applied Financial Economics*, 12(3), 193–202.
- 9 **Kube, N.** (2018). *Daniel Drescher: Blockchain basics: A non-technical introduction in 25 steps: Apress, 2017, 255 pp, ISBN: 978-1-4842-2603-2.*

- 10 **Chaum, D.** (1983). Blind signatures for untraceable payments, *Advances in Cryptology: Proceedings of Crypto 82*, Springer, pp.199–203.
- 11 **Chaum, D., Fiat, A. and Naor, M.** (1990). Untraceable electronic cash, *Advances in Cryptology—CRYPTO’88: Proceedings 8*, Springer, pp.319–327.
- 12 **Law, L., Sabett, S. and Solinas, J.** (1996). How to make a mint: The cryptography of anonymous electronic cash, *Am. UL Rev.*, 46, 1131.
- 13 **Dai, W.** (1998). *B-money*.
- 14 **Peck, M.E.** (2012). Bitcoin: the cryptoanarchists’ answer to cash. How Bitcoin brought privacy to electronic transactions, *IEEE Spectrum*.
- 15 **Rice, M.** (2019). Cryptocurrency: History, advantages, disadvantages, and the future.
- 16 *Top Meme Coins by Market Cap*, <https://www.coingecko.com/en/categories/meme-token#key-stats/>, accessed: 2025-05-13.
- 17 **Buterin, V. et al.** (2013). Ethereum white paper, *GitHub repository*, 1(22-23), 5–7.
- 18 *Ethereum Energy Consumption Index*, <https://digiconomist.net/ethereum-energy-consumption/>, accessed: 2025-06-13.
- 19 *Central Bank Digital Currencies (CBDCs)*, <https://ico.org.uk/about-the-ico/research-reports-impact-and-evaluation/research-and-reports/technology-and-innovation/tch-horizons-and-ico-tech-futures/tch-horizons-report-2024/>, accessed: 2025-06-13.
- 20 *Crypto Market Data*, <https://coinmarketcap.com/>, accessed: 2025-03-11.
- 21 **Katsiampa, P.** (2017). Volatility estimation for Bitcoin: A comparison of GARCH models, *Economics Letters*, 158, 3–6.

- 22 **Kim, J.M., Jun, C. and Lee, J.** (2021). Forecasting the volatility of the cryptocurrency market by GARCH and Stochastic Volatility, *Mathematics*, 9(14), 1614.
- 23 **Trucíos, C.** (2019). Forecasting Bitcoin risk measures: A robust approach, *International Journal of Forecasting*, 35(3), 836–847.
- 24 **Catania, L., Grassi, S. and Ravazzolo, F.** (2018). Predicting the volatility of cryptocurrency time-series, *Mathematical and Statistical Methods for Actuarial Sciences and Finance: MAF 2018*, 203–207.
- 25 **Dyhrberg, A.H.** (2016). Bitcoin, gold and the dollar—A GARCH volatility analysis, *Finance Research Letters*, 16, 85–92.
- 26 **Balcilar, M., Bouri, E., Gupta, R. and Roubaud, D.** (2017). Can volume predict Bitcoin returns and volatility? A quantiles-based approach, *Economic Modelling*, 64, 74–81.
- 27 **Hattori, T.** (2020). A forecast comparison of volatility models using realized volatility: Evidence from the Bitcoin market, *Applied Economics Letters*, 27(7), 591–595.
- 28 **Fakhfekh, M. and Jeribi, A.** (2020). Volatility dynamics of crypto-currencies' returns: Evidence from asymmetric and long memory GARCH models, *Research in International Business and Finance*, 51, 101075.
- 29 **Caporale, G.M. and Zekokh, T.** (2019). Modelling volatility of cryptocurrencies using Markov-Switching GARCH models, *Research in International Business and Finance*, 48, 143–155.
- 30 **Chaim, P. and Laurini, M.P.** (2018). Volatility and return jumps in Bitcoin, *Economics Letters*, 173, 158–163.
- 31 **Baur, D.G. and Dimpfl, T.** (2018). Asymmetric volatility in cryptocurrencies, *Economics Letters*, 173, 148–151.

- 32 **Cheikh, N.B., Zaied, Y.B. and Chevallier, J.** (2020). Asymmetric volatility in cryptocurrency markets: New evidence from smooth transition GARCH models, *Finance Research Letters*, 35, 101293.
- 33 **Guo, Z.Y.** (2022). Risk management of Bitcoin futures with GARCH models, *Finance Research Letters*, 45, 102197.
- 34 **Bergsli, L.Ø., Lind, A.F., Molnár, P. and Polasik, M.** (2022). Forecasting volatility of Bitcoin, *Research in International Business and Finance*, 59, 101540.
- 35 **Korkmaz, S.** (2024). crypto Quotes: Cryptocurrency Market Data in R. R package version 1.3.0.
- 36 **Gu, Z., Lin, D. and Wu, J.** (2022). On-chain analysis-based detection of abnormal transaction amount on cryptocurrency exchanges, *Physica A: Statistical Mechanics and its Applications*, 604, 127799.
- 37 **Bollerslev, T.** (1986). Generalized Autoregressive Conditional Heteroskedasticity, *Journal of Econometrics*, 31(3), 307–327.
- 38 **Taylor, S.J.** (1994). Modeling stochastic volatility: A review and comparative study, *Mathematical Finance*, 4(2), 183–204.
- 39 **Francq, C. and Zakoian, J.M.** (2019). *GARCH Models: Structure, Statistical Inference and Financial Applications*, John Wiley & Sons.
- 40 **Martin, V., Hurn, S. and Harris, D.** (2013). *Econometric Modelling With Time series: Specification, Estimation and Testing*, Cambridge University Press.
- 41 **Engle, R.F., Lilién, D.M. and Robins, R.P.** (1987). Estimating time varying risk premia in the term structure: The ARCH-M model, *Econometrica: journal of the Econometric Society*, 391–407.
- 42 **Elyasiani, E. and Mansur, I.** (1998). Sensitivity of the bank stock returns distribution to changes in the level and volatility of interest rate: A GARCH-M model, *Journal of banking & finance*, 22(5), 535–563.

- 43 **Mouna, A. and Anis, J.** (2016). Market, interest rate, and exchange rate risk effects on financial stock returns during the financial crisis: AGARCH-M approach, *Cogent Economics & Finance*, 4(1), 1125332.
- 44 **Glosten, L.R., Jagannathan, R. and Runkle, D.E.** (1993). On the relation between the expected value and the volatility of the nominal excess return on stocks, *The Journal of Finance*, 48(5), 1779–1801.
- 45 **Koopman, S.J. and Hol Uspensky, E.** (2002). The stochastic volatility in mean model: Empirical evidence from international stock markets, *Journal of Applied Econometrics*, 17(6), 667–689.
- 46 **Chan, J.C. and Jeliazkov, I.** (2009). Efficient simulation and integrated likelihood estimation in state space models, *International Journal of Mathematical Modelling and Numerical Optimisation*, 1(1-2), 101–120.
- 47 **Chan, J.C.** (2017). The stochastic volatility in mean model with time-varying parameters: An application to inflation modeling, *Journal of Business & Economic Statistics*, 35(1), 17–28.
- 48 **Chan, J.C. and Eisenstat, E.** (2015). Marginal likelihood estimation with the cross-entropy method, *Econometric Reviews*, 34(3), 256–285.
- 49 **Fan, Y., Zhang, Y.J., Tsai, H.T. and Wei, Y.M.** (2008). Estimating ‘Value at Risk’ of crude oil price and its spillover effect using the GED-GARCH approach, *Energy Economics*, 30(6), 3156–3171.
- 50 **Hung, J.C., Lee, M.C. and Liu, H.C.** (2008). Estimation of value-at-risk for energy commodities via fat-tailed GARCH models, *Energy Economics*, 30(3), 1173–1191.
- 51 **Geweke, J. and Amisano, G.** (2011). Hierarchical Markov normal mixture models with applications to financial asset returns, *Journal of Applied Econometrics*, 26(1), 1–29.



CURRICULUM VITAE

Name SURNAME: IRFAN CANER KAYA

EDUCATION:

- **B.Sc.:** 2014, Hacettepe University, Engineering Faculty, Industrial Engineering
- **M.Sc.:** 2017, Bilkent University, Graduate Program, Industrial Engineering

PROFESSIONAL EXPERIENCE AND REWARDS:

- 2021-2024 Researcher at Turkish Management Sciences Institute (TUBITAK TUSSIDE)
- 2024-Continue Researcher at TUBITAK MARMARA RESEARCH CENTER

PUBLICATIONS, PRESENTATIONS AND PATENTS ON THE THESIS:

- **Kaya, I.C.** (2025). Comparative Analysis OF GARCH and Stochastic Volatility Models for Capturing The Price Dynamics of Bitcoin and Ethereum. *INTERNATIONAL YILDIRIM BAYEZID SCIENTIFIC RESEARCH AND INNOVATION SYMPOSIUM-I*, May 09-10, 2025, Bursa, Turkey.